City of Morro Bay and
Cayucos Sanitary District

OFFSHORE MONITORING AND REPORTING PROGRAM

THIRD QUARTER RECEIVING–WATER SURVEY

SEPTEMBER 2017

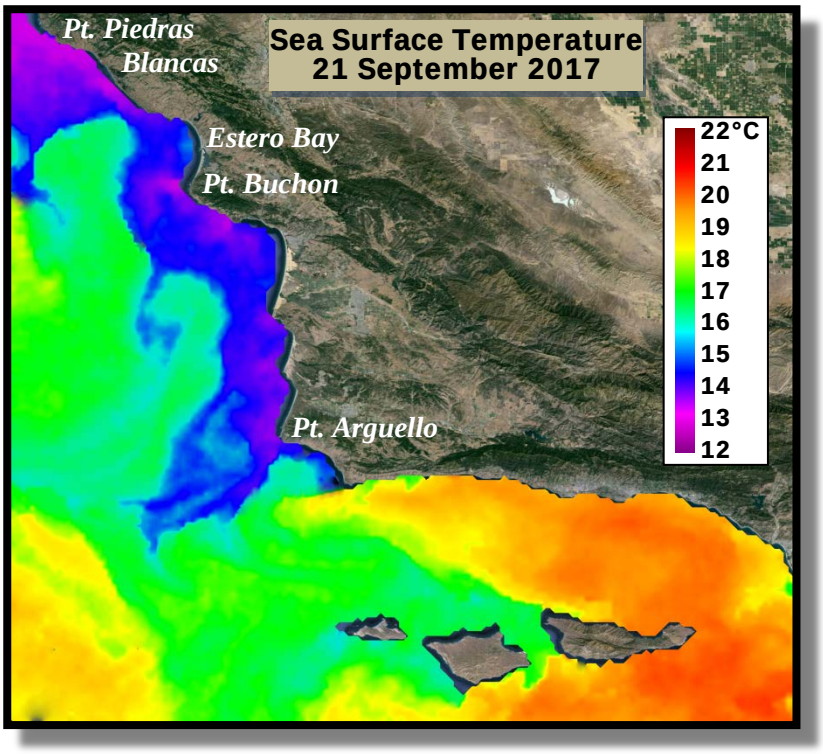

Marine Research Specialists
4744 Telephone Rd Ste 3 PMB 315
Ventura, California 93003

Report to the

City of Morro Bay and
Cayucos Sanitary District

955 Shasta Avenue
Morro Bay, California 93442
(805) 772-6272

OFFSHORE MONITORING AND REPORTING PROGRAM

THIRD QUARTER RECEIVING–WATER SURVEY

SEPTEMBER 2017

Prepared by

Douglas A. Coats

Marine Research Specialists

4744 Telephone Rd Ste 3 PMB 315
Ventura, California 93003

Telephone: (805) 644-1180
E-mail: Marine@Rain.org

October 2017

marine research specialists
4744 Telephone Rd., STE 3 PMB 315 • Ventura, CA 93003 • 805-644-1180

John Gunderlock
Wastewater & Collection Systems Supervisor
City of Morro Bay
955 Shasta Avenue
Morro Bay, CA 93442

27 October 2017

Reference: Third Quarter Receiving-Water Survey Report – September 2017

Dear Mr. Gunderlock:

The attached report presents results from a quarterly receiving-water survey conducted on Tuesday, 19 September 2017. The survey was conducted in accordance with the requirements of the NPDES permit issued to the City and District for discharge of treated wastewater to Estero Bay. The report evaluated compliance with permit limitations and assessed the effectiveness of effluent dispersion within receiving waters. Quantitative analyses of continuous instrumental measurements and qualitative visual observations confirmed that the wastewater discharge complied with the receiving-water limitations specified in the permit, and with the objectives of the California Ocean Plan.

The offshore measurements confirmed that the diffuser structure and treatment plant continued to operate at a high level of performance. The measurements delineated a diffuse discharge plume containing low organic loads within a localized region south of the discharge point. Dilution within the plume exceeded expectations based on modeling and outfall design criteria.

Contact the undersigned if you have questions regarding the attached report.

Sincerely,

Douglas A. Coats

Douglas A. Coats
Program Manager

I certify under penalty of law that this document and all attachments were prepared under my direction or supervision in accordance with a system designed to assure that qualified personnel properly gather and evaluate the information submitted. Based on my inquiry of the person or persons who manage the system, or those persons directly responsible for gathering the information, the information submitted is, to the best of my knowledge and belief, true, accurate and complete. I am aware that there are significant penalties for submitting false information, including the possibility of fine and imprisonment for knowing violations.

Mr. John Gunderlock
Wastewater/Collections System Supervisor
City of Morro Bay/Cayucos CSD Wastewater Treatment Plant

Date: 10/27/17

TABLE OF CONTENTS

LIST OF FIGURES

LIST OF TABLES

INTRODUCTION

The City of Morro Bay and the Cayucos Sanitary District (MBCSD) jointly own the wastewater treatment plant (WWTP) operated by the City of Morro Bay. In March 1985, Region IX of the U.S. Environmental Protection Agency (USEPA) and the Central Coast California Regional Water Quality Control Board (RWQCB) issued the first National Pollutant Discharge Elimination System (NPDES) permit to the MBCSD. The permit incorporated partially modified secondary treatment requirements for the plant's ocean discharge. The permit has been re-issued three times, in March 1993 (RWQCB-USEPA 1993ab), December 1998 (RWQCB-USEPA 1998ab), and January 2009 (RWQCB-USEPA 2009). The September 2017 field survey described in this report was the thirty-fifth receiving-water survey conducted under the current permit.

The NPDES discharge permit requires seasonal monitoring of offshore receiving-water quality with quarterly surveys. This report summarizes the results of sampling conducted on 19 September 2017. Specifically, this third-quarter survey captured ambient oceanographic conditions along the central California coast during the late summer season. The survey's measurements were used to assess the discharge's compliance with the objectives of the California Ocean Plan (COP) and the Central Coast Basin Plan (RWQCB 1994) as promulgated by the receiving-water limitations specified in the NPDES discharge permit.

The monitoring objectives were achieved by empirically evaluating tabulations of instrumental measurements and standard field observations. In addition to the traditional, vertical water-column profiles, instrumental measurements were used to generate horizontal maps from high-resolution data gathered by towing a CTD[1] instrument package repeatedly over the diffuser structure. This allowed for a more precise delineation of the plume's lateral extent.

SURVEY SETTING

The MBCSD treatment plant is located within the City of Morro Bay, which is situated along the central coast of California halfway between Los Angeles and San Francisco. Effluent is carried from the onshore treatment plant through a 1,450-m long outfall pipe, which terminates at a diffuser structure on the seafloor 827 m from the shoreline within Estero Bay (Figure 1). The diffuser structure extends an additional 52 m toward the northwest from the outfall terminus and consists of 34 ports that are hydraulically designed to create a turbulent ejection jet that rapidly mixes effluent with receiving seawater upon discharge. Currently, six of the diffuser ports are closed, thereby improving effluent dispersion by increasing the ejection velocity from the remaining 28 ports distributed along a 42-m section of the diffuser structure.

Following discharge from the diffuser ports, additional turbulent mixing occurs as the buoyant plume of dilute effluent ascends through the water column. Most of this buoyancy-induced mixing occurs within a zone of initial dilution (ZID), whose lateral reach in modeling studies extends 15.2 m from the centerline of the diffuser structure. Beyond the ZID, energetic waves, tides, and coastal currents within Estero Bay further disperse the dilute effluent within the open-ocean receiving waters. Both vertical hydrocasts and horizontal tow surveys are conducted around the diffuser structure to assess the efficacy of the diffuser, to define the lateral extent of the discharge plume, and to evaluate compliance with the NPDES permit limitations.

[1] Conductivity, temperature, and depth (CTD)

Figure 1. Location of the Receiving-Water Survey Area

Near the diffuser, prevailing flow generally follows bathymetric contours that parallel the north-south trend of the adjacent coastline. Because of the rapid initial mixing achieved within 15 m of the diffuser structure, impingement of unmixed effluent onto the adjacent coastline, 827 m away, is highly unlikely. Nevertheless, in the event of a failure in the treatment plant's disinfection system, collection and analysis of water samples at the eight surfzone-sampling stations shown in Figure 1 would be conducted to monitor for potential shoreline impacts. These surfzone samples would be analyzed for total and fecal coliform, and enterococcus bacterial densities.

Areas of special concern, such as the Morro Bay National Estuary and the Monterey Bay National Marine Sanctuary, are not affected by the discharge because they are even more distant from the outfall location. For example, the southern boundary of the Monterey Bay National Marine Sanctuary is located 38 km to the north, while the entrance to the Morro Bay National Estuary lies 2.8 km south. The southerly orientation of the mouth of the Bay, and the presence of Morro Rock 2 km to the south, serve to further limit direct seawater exchange between the discharge point and the Bay (Figure 1).

SAMPLING LOCATIONS

As shown in Figure 2, the offshore sampling pattern consists of six fixed offshore stations located within 100 m of the outfall diffuser structure. The red ⊙ symbols in the Figure indicate the target locations of the sampling stations (Table 1). The stations are situated at three distances relative to the center of the diffuser structure, and lie along a north-south axis at the same water depth (15.2 m) as the center of the diffuser. Depending on the direction of the local oceanic currents at the time of sampling, the discharge may influence one or more of these stations. The up-current stations on the opposite side of the diffuser then act as reference stations. Comparisons between the water properties at these antipodal stations quantify departures from ambient seawater properties caused by the discharge and allow compliance with the NPDES discharge permit to be determined.

The finite size of the diffuser is an important consideration in the assessment of wastewater dispersion close to the discharge. Although the discharge is considered a "*point source*" for modeling and regulatory purposes, it does not occur at a single isolated point of infinitesimal size. Instead, the discharge is distributed along a 42 m section of the seafloor, and, ultimately, the amount of wastewater dispersion at a given point in the water column is dictated by its distance from the closest diffuser port, rather than its distance from the center of the diffuser structure. This "*closest approach*" distance can be considerably less than the centerpoint distance normally cited in modeling studies (compare the last two columns of Table 1).

Another important consideration for compliance evaluation is the ability to determine the actual location of the measurements. Discerning small spatial separations within the compact sampling pattern only became feasible after the advent of Differential Global Positioning Systems (DGPS). The accuracy of traditional navigation systems such as LORAN or standard GPS is typically ±15 m, a span equal to half the total width of the ZID itself. DGPS incorporates a second signal from a fixed, land-based beacon that continuously transmits position errors in standard GPS readings to the DGPS receiver aboard the survey vessel. Real-time correction for these position errors provides an extremely stable and accurate offshore navigational reading with position errors of no more than 2 m, and often with sub-meter accuracy.

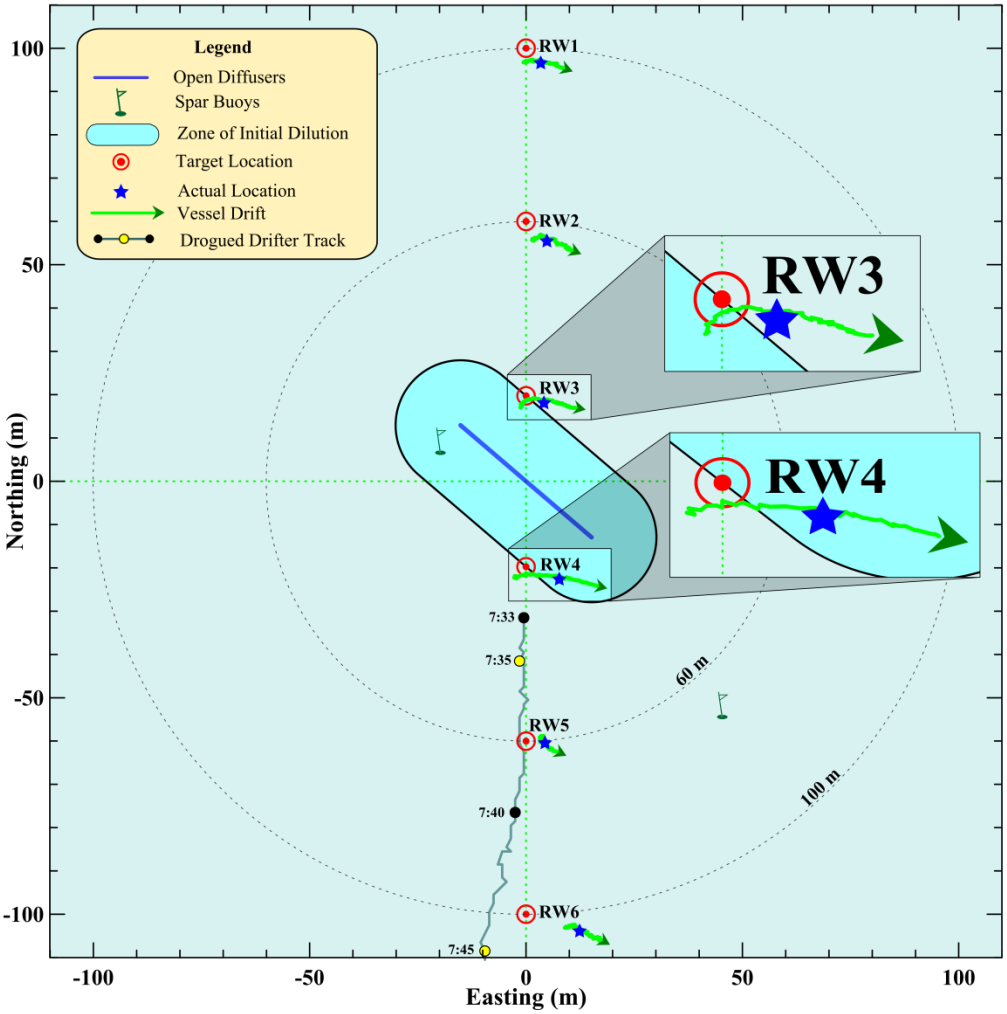

Figure 2. Station Locations

Table 1. Target Locations of the Receiving-Water Monitoring Stations

Station	Description	Latitude	Longitude	Center Distance[2] (m)	Closest Approach Distance[3] (m)
RW1	Upcoast Midfield	35° 23.253' N	120° 52.504' W	100	88.4
RW2	Upcoast Nearfield	35° 23.231' N	120° 52.504' W	60	49.4
RW3	Upcoast ZID	35° 23.210' N	120° 52.504' W	20	15.0
RW4	Downcoast ZID	35° 23.188' N	120° 52.504' W	20	15.0
RW5	Downcoast Nearfield	35° 23.167' N	120° 52.504' W	60	49.4
RW6	Downcoast Midfield	35° 23.145' N	120° 52.504' W	100	88.4

[2] Distance to the center of the open diffuser section
[3] Distance to the closest open diffuser port

During a diver survey in July 1998, the survey vessel's new DGPS navigation system, consisting of a Furuno™ GPS 30 and FBX2 differential beacon receiver, was used to precisely determine the position of the open section of the diffuser structure (MRS 1998) and establish the target locations for the receiving-water monitoring stations shown in Figure 2 and listed in Table 1. Presently, the use of two independent DGPS receivers aboard the survey vessel allows access to two separate land-based beacons for navigational intercomparison, ensuring extremely accurate and uninterrupted navigational reports.

Recording of DGPS positions at one-second intervals allows precise determination of sampling locations throughout the vertical CTD profiling conducted at the six individual stations, as well as during the tow survey. Knowledge of the precise location of individual CTD measurements relative to the diffuser is critical for accurate interpretation of the water-property fields. During vertical-profile sampling, for example, the actual measurement locations rarely coincide with the target coordinates listed in Table 1 because winds, waves, and currents induce unavoidable horizontal offsets (drift). Even during quiescent metocean[4] conditions, the residual momentum of the survey vessel as it approaches the target locations can create perceptible offsets. Using DGPS however, these offsets can be quantified, and the vessel location can be precisely tracked throughout sampling at each station.

The September 2017 hydrocasts were conducted progressing from south to north, beginning with Station RW6. The magnitude of the drift at each of the six stations during the September 2017 survey is apparent from the length of the green tracklines in Figure 2. The tracklines trace the horizontal movement of the CTD as it was lowered to the seafloor at each station. Their lengths and offsets from the target locations reflect the overall station-keeping ability during the September 2017 survey.

The time it took the CTD to traverse the water column to the seafloor, which averaged 1 min 11 s, was consistent among stations, while the lateral distance traversed by the instrument package varied considerably among the stations (Figure 2). Although the drift was toward the southeast at each station, its extent ranged from 4 m at Station RW5 to 19 m at Station RW4. The lateral movement of the CTD at any given time is often determined by a complex interplay between the external influences of winds and currents, and the vessel's residual momentum immediately prior to each downcast. For example, the increased southeastward drift at Station RW4 arose from the vessel's greater residual momentum as it approached the station from the northwest. The slower approach at most other stations combined with a light onshore breeze out of the northwest transported the vessel slowly toward the southeast during the downcasts.[5] Although the strong southward current flow, reflected in the drogued-drifter trajectory in Figure 2,[6] also undoubtedly introduced some curvature in the CTD's movement during the downcasts, its influence was secondary to the influences of wind and vessel approach.

Regardless of the cause, detailed knowledge of the CTD's movement during downcasts is important for the interpretation of the water-quality measurements. Because the target locations for Stations RW3 and RW4 lie along the ZID boundary (viz., the red ⊙ symbols in the insets in Figure 2), knowledge of the CTD's location during the downcasts at those stations is especially important in the compliance evaluation. This is because the receiving-water limitations specified in the COP only apply to measurements recorded along or beyond the ZID boundary, where initial mixing is assumed complete.

[4] Meteorological and oceanographic conditions include winds, waves, tides, and currents.
[5] Refer to the wind measurements in Table 4 later in this report.
[6] Refer to the partial drogued-drifter track shown in Figure 2 and the full track in Figure 3 later in this report.

During the September 2017 survey, the upper 5 m of data collected at Station RW3 was not subject to a compliance assessment because the CTD was located within the ZID during the initial portion of the downcast. The CTD traversed the ZID boundary as it was lowered through the water column. It was first briefly transported toward the north (from vessel momentum), and then toward east southeast (refer to the upper right inset in Figure 2). Thus, only data recorded below 5 m Station RW3 were subject to a compliance analysis. Similarly, most data collected at Station RW4 were not subject to a compliance assessment because the CTD traversed the ZID boundary when it reached a depth of 4 m, shortly after the downcast was initiated at that station (lower right inset in Figure 2).

Compliance assessments notwithstanding, measurements acquired within the ZID lend valuable insight into the outfall's effectiveness at dispersing wastewater. For example, low dilution rates and concentrated effluent throughout the ZID would indicate potentially damaged or broken diffuser ports. Analysis of the outfall's operation over the past two and a half decades, however, demonstrates that it has consistently maintained a high level of effectiveness in effluent dispersal. In fact, without the occasional measurements recorded within the ZID due to vessel drift, the extremely dilute discharge plume might remain undetected within all the vertical profiles collected during a given survey.

It has not always been possible to determine which measurements were subject to permit limits among hydrocasts near the ZID boundary, however. For example, prior to 1999 and before the advent of DGPS, CTD locations could not be determined with sufficient accuracy to establish whether the average ZID station position was located within the ZID, much less, how the CTD was moving laterally during the hydrocast. Because of these navigational limitations, sampling was presumed to occur at a single, imprecisely determined, horizontal location. Federal and state reporting of monitoring data still mandates identification of a single position for all of the CTD data collected at a particular station. Thus, for regulatory reporting, and for consistency with past surveys, the September 2017 survey also identifies a single sampling location for each station. These average station positions are identified by the blue stars in Figure 2, and are listed in Table 2 along with their distances from the diffuser structure.

Table 2. Average Position of Vertical Profiles during the September 2017 Survey

	Time (PDT)				Closest Approach	
Station	**Downcast**	**Upcast**	**Latitude**	**Longitude**	**Range[7] (m)**	**Bearing[8] (ºT)**
RW1	9:47:47	9:48:47	35° 23.251' N	120° 52.502' W	85.8	12
RW2	9:44:23	9:45:31	35° 23.229' N	120° 52.501' W	47.1	25
RW3	9:40:58	9:42:17	35° 23.209' N	120° 52.501' W	**16.6[9]**	41
RW4	9:36:28	9:37:40	35° 23.187' N	120° 52.499' W	**12.1[10]**	218
RW5	9:33:13	9:34:20	35° 23.166' N	120° 52.501' W	48.6	193
RW6	9:29:37	9:30:55	35° 23.143' N	120° 52.496' W	90.9	182

[7] Distance from the closest open diffuser port to the average profile location
[8] Angle measured clockwise relative to true north from the closest diffuser port to the average profile location
[9] Some of the CTD measurements were located within the ZID boundary (refer to the upper right inset in Figure 2).
[10] Most of the CTD measurements were located within the ZID boundary (refer to lower right inset in Figure 2).

OCEANOGRAPHIC PROCESSES

The trajectory of a satellite-tracked drogued drifter measured oceanic flow throughout the September 2017 survey (Figure 3). Modeled after the curtain-shade design of Davis et al. (1982) and drogued at mid-depth (7 m), a drifter has been deployed during each of the quarterly water column surveys conducted over the past two decades. In this configuration, oceanic flow rather than surface wind dictates the drifter's trajectory, which provides a good indication of the plume's movement after discharge, except when the flow field exhibits strong vertical shear.

During the September 2017 survey, the drifter was deployed near the diffuser structure at 7:33 AM, and was recovered at 10:13 AM at a location 980 m south southeast (169°T[11]) of its original release point (red dots in Figure 3). However, the slightly serpentine route of the drifter indicated that the currents that transported the drifter varied during its deployment.

For the first half-hour after deployment, the drifter travelled at a rapid pace of 10.3 cm/sec [12] along a 167 m path slightly west of the generally southward transport direction. At 8:00 AM, the trajectory initiated a slight change in direction toward the east for 50 minutes, followed by another brief 20-minute period with a slight westerly drift component again. Lastly, at 9:10, and well before the vertical profiling was initiated, the mid-depth current flow was redirected toward the southeast for the remainder of the drifter's deployment.

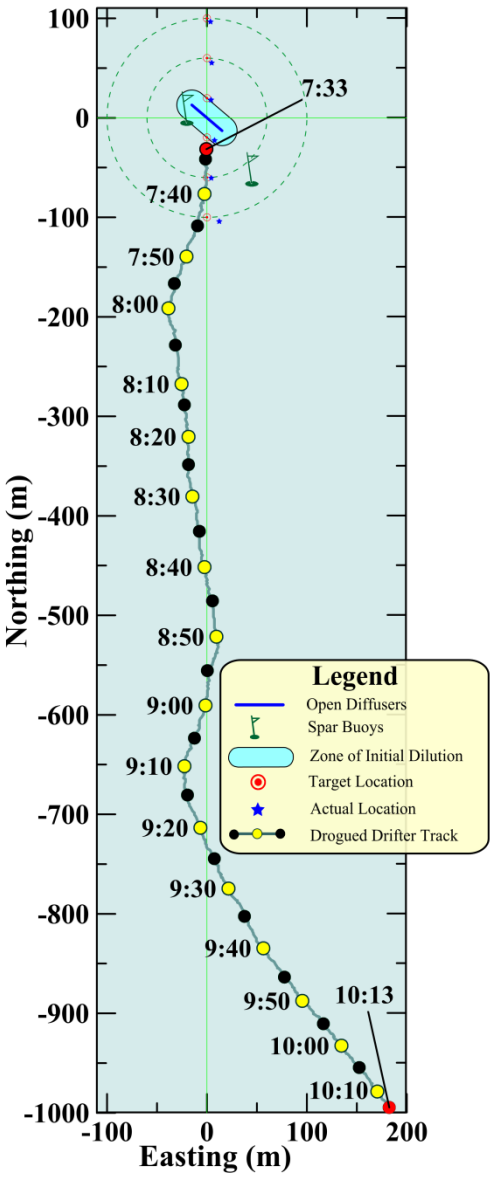

Figure 3. Drogued Drifter Trajectory

The circuitous drifter track demonstrated that the mid-depth oceanic current varied throughout the survey. The transport speed was relatively consistent throughout the survey, as is apparent from the uniform spacing between the yellow and black dots in Figure 3, which show the drifter's progress at five- and ten-minute intervals. However, because of heading changes, the cumulative distance traversed by the drifter was actually 1,040 m. After accounting for the additional 60 m of travel, the 10.8 cm/s[13] average flow speed characterized the rate at which the effluent plume was transported laterally during the September 2017 survey. This plume transport rate was greater than that observed during most prior surveys, and indicated that effluent would have experienced only a brief, 2.3-minute residence time within the ZID at the time of this survey.

[11] Direction measured clockwise relative to true (rather than magnetic) north
[12] 0.2 kt
[13] 0.21 kt

The drifter trajectory accurately depicted the southward transport of the effluent plume during the survey, as indicated by the southerly offset of the plume's salinity signature that was delineated during the tow surveys.[14] This consistency in directional offset suggests that the drifter's movement accurately captured flow that was representative of plume transport throughout the mid and lower water column. However, when the water column is strongly stratified, as was the case during the September 2017 survey, vertical countercurrents can form above and below a sharply defined thermocline.[15] It is likely that the flow within the surface mixed layer departed from the mid-depth flow measured by the drifter.

In contrast to vertically sheared flow that is typical of strongly stratified conditions during upwelling, barotropic (vertically uniform) flow is a hallmark of tidal forcing. However, it is unlikely that the flood tide that prevailed throughout the survey (Figure 4) significantly contributed to the southward flow observed at mid-depth. Flood tides normally induce a uniform shoreward (northward) component of flow throughout the water column. Instead, as is typical of current dynamics within the survey area, a variety of oceanographic processes combine to establish the local flow conditions near the diffuser structure. These other forces include regionally generated upwelling winds as well as distant remote processes, such as large-scale along-shore pressure gradients or the passing of large eddies embedded within the California Current.

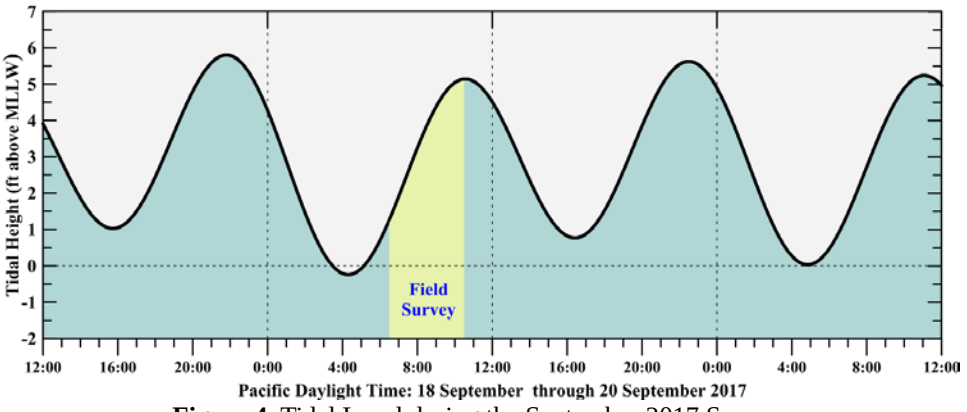

Figure 4. Tidal Level during the September 2017 Survey

Normally, along this section of coastline, currents within the survey area are largely determined by the prevailing wind field. Strong and steady northwesterly winds cause upwelling within the water column and produce a system of vertical countercurrents (Figure 5). In the upper water column, net wind-driven Ekman transport occurs at a 90º angle to the prevailing wind.[16] As a result, warm ocean waters within the surface mixed layer are driven offshore (southwestward) in response to the along-shore winds (toward the southeast). Near the coast, these warm surface waters are replaced by deep, cool, nutrient-rich waters that well up from below. The upwelled waters originate farther offshore and move shoreward (northeastward) along the seafloor

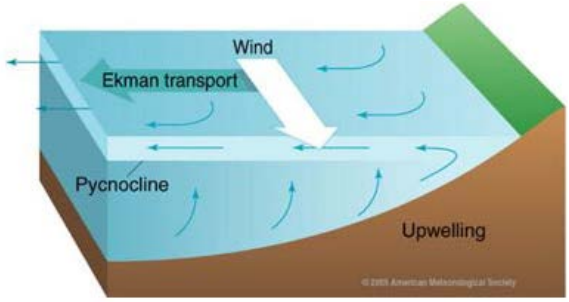

Figure 5. Schematic of Upwelling Processes

[14] Refer to Figures 9b and 10b later in this report.

[15] At the northern Stations RW1, RW2, and RW3 (Figure 8abc later in this report) ambient seawater properties changed rapidly beneath a 7-m thick surface mixed layer that extended downward from the sea surface. Within the 6-m thick transition zone beneath the mixed layer, most seawater properties rapidly declined to levels typical of the 3-m thick benthic layer that moved shoreward along the seafloor.

[16] http://oceanmotion.org/html/background/upwelling-and-downwelling.htm

as part of the upwelling process. Thus, upwelling establishes a vertically sheared current flow within the survey area.

The onset of these upwelling-dominated processes normally begins with a rapid intensification of southeastward-directed winds along the central coast during late March and or early April as shown by the positive (blue) upwelling indices in Figure 6. This transition to more persistent southeastward winds is initiated by the stabilization of a high-pressure field over the northeastern Pacific Ocean. Clockwise winds around this pressure field drive prevailing northwesterly winds along the central California coast. The September 2017 survey was conducted during an unusually strong late-season pulse of upwelling winds that had an index near 150, indicating that upwelling was more intense than during surveys conducted over the prior three years (refer to the inset containing the last yellow diamond in Figure 6).

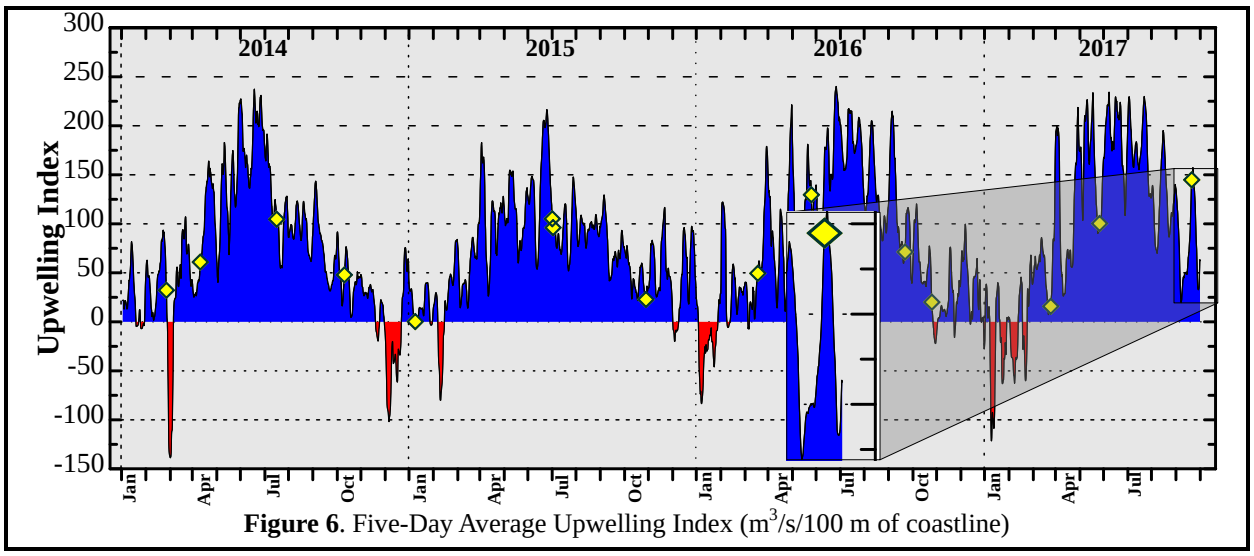

Figure 6. Five-Day Average Upwelling Index ($m^3/s/100$ m of coastline)

Nevertheless, some degree of upwelling is almost always present during offshore surveys (other yellow diamonds in Figure 6). Throughout most of the year, the nutrient-rich seawater brought to the sea surface near the coast by upwelling enables phytoplanktonic blooms that are the foundation of the productive marine fishery found along the central California coast. The vertical counterflow associated with persistent upwelling conditions also enhances vertical stratification of the water column. The influx of cold dense water at depth produces a thermocline that is commonly maintained throughout summer and into early fall.

During late fall and winter, upwelling is typically weak, and occasionally downwelling events, indicated by the negative (red shaded) indices in Figure 6, occur when passing storms temporarily reverse the normal wind pattern and drive surface waters shoreward. As the surface waters approach the coastline, they downwell, producing nearly uniform seawater properties throughout the water column. An unusual series of severe winter storms at the beginning of 2017 produced multiple downwelling events (refer to the red downward excursions in the upwelling index during January and February 2017 in Figure 6).

In contrast, the strong and sustained winds that prevailed before and during the September 2017 survey produced a pattern of sea surface temperatures indicative of intense upwelling within the central-coast oceanographic region. This upwelling pattern was captured by the satellite image shown on the cover of this report. The image was recorded by infrared sensors on one of NOAA's polar orbiting satellites during a period of relatively cloudless skies two days after the survey. The presence of pools of cooler, upwelled water is visually apparent immediately adjacent to the south-central coastline (dark -blue and magenta shading). The large 6°C difference between these sea-surface temperatures and temperatures farther

offshore (in green and yellow) demonstrate that intense upwelling had a profound effect on oceanographic conditions throughout the region.

METHODS

The 38 ft F/V *Bonnie Marietta*, owned and operated by Captain Mark Tognazzini of Morro Bay, served as the survey vessel on Friday, 19 September 2017. Douglas Coats of Marine Research Specialists (MRS) supervised scientific operations as Chief Scientist, and provided data-acquisition and navigational support during the survey. He also assisted with the deployment and recovery of the CTD and drifter, and he collected meteorological measurements at each station. Crewmember William Skok managed deck operations and collected the Secchi depth measurements at each station.

Auxiliary Measurements

Auxiliary measurements and observations were collected at each of the six stations after completion of the vertical profiling phase of the survey. Standard observations of weather and sea conditions, and beneficial uses, were augmented by visual inspection of the sea surface for floating particulates, oil sheens, and discoloration potentially related to effluent discharge. Other auxiliary measurements collected at each station included wind speeds and air temperatures measured with a handheld Holdpeak 866B Digital Thermo-Anemometer, and oceanic flow measurements made throughout the survey area using the aforementioned drogued drifter.

Additionally, at all six stations, a Secchi disk was lowered through the water column to determine its depth of disappearance. Secchi depths provide a visual measure of near-surface turbidity or water clarity. The depth of disappearance is inversely proportional to the average amount of organic and inorganic material suspended along a line of sight in the upper water column. As such, Secchi depths measure natural light penetration, which can be limited by increased suspended particulate loads from plankton blooms, onshore runoff, seafloor sediment resuspension, and wastewater discharge. They are also biologically meaningful because the depth of the euphotic zone, where most oceanic photosynthesis occurs, is limited to approximately twice the Secchi depth.

Instrumental Measurements

A Sea Bird Electronics SBE-19plusV2 Seacat CTD instrument package collected measurements of conductivity, temperature, light transmittance, dissolved oxygen (DO), pH, and pressure during the September 2017 survey. The six seawater properties used to assess receiving-water quality in this report were derived from the continuously recorded output from the CTD's probes and sensors. Although pressure-housing limitations confine the CTD to depths less than 680 m (Table 3), this is well beyond the

Table 3. CTD Specifications

Component	Units	Range	Accuracy	Resolution
Housing (19p-1a; Acetron Plastic)	m	0 to 680	—	—
Pump (SBE 5P)	—	—	—	—
Pressure (19p-2h; Strain-Gauge)	dBar	0 to 680	±1.7	± 0.10
Conductivity	Siemens/m	0 to 9	± 0.0005	± 0.00005
Salinity	‰	0 to 58	± 0.004	± 0.0004
Temperature	ºC	–5 to 35	± 0.005	± 0.0001
Transmissivity (WETLabs C-Star)[17]	%	0 to 100	± 0.3	± 0.03
Oxygen (SBE 43)	% Saturation	0 to 120	± 2	—
pH (SBE 18)	pH	0 to 14	± 0.1	—

[17] 25-cm path length of red (650 nm) light

maximum depth of the deepest station in the outfall survey. The entire CTD was returned to the factory in January 2015 for full calibration and servicing. The transmissometer and DO probe were returned to the manufacturer in January 2016 for further servicing, repair, and calibration.

The precision and accuracy of the various probes, as reported in manufacturer's specifications, are listed in Table 3. Salinity (‰) was calculated from conductivity measurements reported in units of Siemens/m. Density was derived from contemporaneous temperature (°C) and salinity data, and was expressed as 1000 times the specific gravity minus one, which is a unit of sigma-T (σ_t).

Assessments of all three of the physical parameters (salinity, temperature, and density) helped determine the lateral extent of the effluent plume during the towing phase of the survey. Additionally, during the vertical-profiling phase, they quantified layering, or vertical stratification and stability of the water column, which determines the behavior and dynamics of the effluent as it mixes with seawater within and beyond the ZID. Data on the three remaining seawater properties, light transmittance (water clarity), hydrogen-ion concentration (acidity/alkalinity – pH), and dissolved oxygen (DO), further characterized the receiving waters, and were used to assess compliance with water-quality criteria. Light transmittance was measured as a percentage of the initial intensity of a transmitted beam of light detected at the opposite end of a 0.25-m path. Transmissivity readings are reported relative to 100% transmission in air, so the maximum theoretical transmission in (pure) water is expected to be 91.3%.

Before beginning the mid-depth tow survey at 7:46 AM, the CTD was deployed beneath the sea surface for a five-minute equilibration period as the vessel was positioned for the first transect. Prior to deployment, the CTD package had been configured for horizontal towing with forward-looking probes. The protective cage around the CTD was fitted with a horizontal stabilizer wing and a depth-suppression weight was added to the towline to achieve near constant-depth tows.

Nine transects of mid-depth data were collected at an average depth of 9.5 m and an average speed of 1.81 m/s over the span of 40 minutes (blue-green lines in Figure 7). Subsequently, at 8:29 AM, nine additional passes were made with the CTD at an average depth of 4.2 m (orange lines). During this 43-minute shallow tow, vessel speed averaged 1.71 m/s.

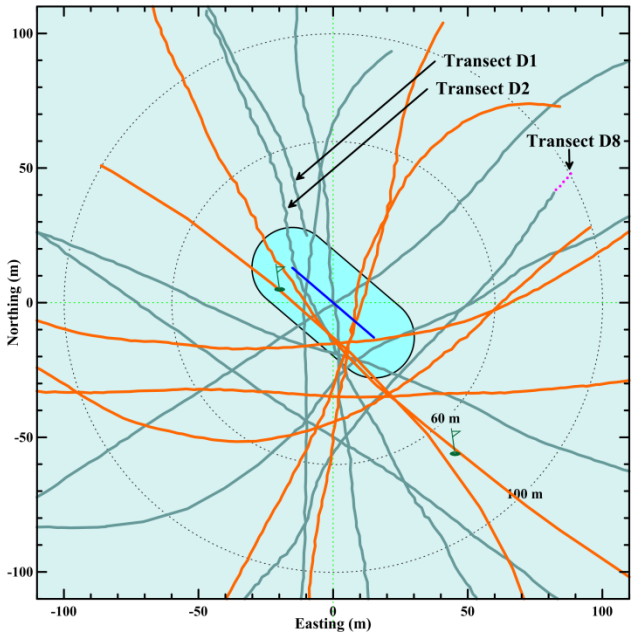

Figure 7. CTD Tracklines during the September 2017 Tow Surveys

At the observed towing speeds and the 4 Hz sampling rate, at least 2.2 CTD measurements were collected for each meter traversed. This complies with the NPDES discharge permit requirement for minimum horizontal resolution of at least one sample per meter during at least five passes around and across the ZID at two separate depths, one within the surface mixed layer and one at mid-depth within the thermocline. Contemporaneous navigation fixes recorded aboard the survey vessel were adjusted for CTD setback and aligned with time stamps on the internally recorded CTD data. The resulting data for the six

seawater properties were then processed to produce horizontal maps within the upper and sub-thermocline portions of the water column.[18]

At 9:12 AM, following completion of the last shallow transect, the CTD package was brought aboard the survey vessel and reconfigured for vertical profiling. The CTD was redeployed at 9:26 AM, and was held beneath the surface for three minutes as the vessel was repositioned over Station RW6. The CTD was then raised to within 0.5 m of the sea surface and profiling commenced. The CTD was lowered at a continuous rate of speed to the seafloor. Measurements at all six stations were collected during a single deployment of the CTD package by towing it below the ocean surface while transiting between adjacent stations.

Quality Control

During the vertical-profiling and horizontal-towing phases of the survey, real-time data were monitored for completeness and range acceptability. Although real-time monitoring indicated that the recorded properties were complete and within acceptable coastal seawater ranges,[19] subsequent post-processing revealed events that impacted portions of the data, resulting in the adjustment or exclusion of these data prior to initiating the compliance analysis. As in the case of most prior surveys, review of the tow data revealed that the CTD changed depth when the vessel executed a turn at the end of each transect. These vertical offsets in CTD depth are introduced by changes in vessel speed and direction that are instituted to realign the vessel between each transect. Because of the complex interaction between turn radius, vessel speed, and CTD depth, the CTD's target depth cannot always be maintained at these times.

Because the discharge-related anomalies used in the compliance analysis are identified by comparing the amplitudes of measurements acquired at the same depth level, the ability to resolve anomalies with statistical certainty is compromised when data from different depth levels are combined in the horizontal maps. This is particularly true when the water column is strongly stratified, as was the case during the September 2017 survey. However, only a small portion of one transect (D8) exhibited an unacceptable depth offset due to turning within the 100-m survey area (purple dotted line in Figure 7).

Nevertheless, three other types of events impacted data collected during the tow-survey and vertical-cast phases, and resulted in the further exclusion or correction of some of the data. First, an intermittent short in the power feed to both the navigational systems resulted in the loss of all position information on seven separate occasions. When the initial interruption was experienced during transit to the survey site, the decision was made to conduct two additional transects at each depth level to ensure adequate spatial coverage if some of the data was subsequently found to be unusable. That navigational interruption, and another one, occurred when surveying was not taking place, and therefore, did not affect data analysis. Additionally, three of the navigational gaps were brief and occurred in the middle of Transects D6, S4, and S5. In those cases, the CTD location could be reliably estimated by linearly interpolating between valid location information that was available before and after the gap. An additional brief navigational gap occurred during the downcast at Station RW1. As in the tow-survey cases, the CTD location was reliably estimated through interpolation.

The remaining navigational gap occurred during the first mid-depth tow transect (D1).[20] In contrast to the other navigational interruptions, vessel locations could not be reliably estimated during the first half of the transect, and all of that data was eliminated from the analysis. Vessel location could not be linearly

[18] Figures 9 and 10 later in this report
[19] Field sampling protocols employed during the survey generally followed the field operations manual for the Southern California Bight Study (SCBFMC 2002), which includes CTD cast-acceptability ranges listed in Table 2 of the manual.
[20] See the foreshortened D1 Transect in Figure 7 that was truncated south of the northern boundary of the ZID.

interpolated because the interruption started well before the transect began at the southern extreme of the survey area. The absence of a valid location measurement near the beginning of the transect precluded linear interpolation within the gap.

Additionally, a second type of event compromised the usefulness of the CTD data collected during the early portions of the mid-depth tow surveys. The pH sensor experienced an unusually extended equilibration period. As a result, the soak period was too brief to provide full equilibration, and pH readings were artificially elevated during the first portion of Transect D1. Thus, the initial portion of Transect D1 would have been excluded for its inaccurate pH measurements had it not been excluded because of the lack of navigational data. Steadily declining pH elevation was also observed during post-processing of Transects D2 and D3, but because the overestimate was small (0.05 pH units), these unaltered data were retained in the analysis. Nevertheless, these very slight instrumental anomalies became apparent in the horizontal pH map.[21]

The third type of event that resulted in the exclusion of data was due to slight changes in overall tow depth during shallow tow Transects S1 and S3. Adjustments to towline length were made during these transects to attain an optimal shallow tow depth. However, because of the stratification, the slight depth changes negatively impacted the ability to resolve lateral variations. As a result, these two shallow transects were excluded from the analysis.

Exclusion of portions of tow data did not adversely affect the compliance analysis, however. The remaining transects were long enough to fully encompass the 100-m survey area surrounding the diffuser structure. Specifically, the tow data that was included in the compliance analysis, shown by the solid orange and blue-green lines in Figure 7, met the permit monitoring requirement of at least five passes near the diffuser structure at each tow depth.

RESULTS

The third-quarter receiving-water survey was conducted on the morning of Tuesday, 19 September 2017. The receiving-water survey commenced at 7:32 AM with the deployment of the drogued drifter. Over the course of the ensuing two hours and forty minutes, offshore observations and measurements were collected as required by the NPDES monitoring program. The survey ended at 10:13 AM with the retrieval of the drogued drifter. Collection of required visual observations of the sea surface was generally unencumbered throughout the survey.

Auxiliary Observations

On the morning of 19 September 2017, skies were clear, with a sustained gentle alongshore breeze out of the northwest (Table 4). Auxiliary observations were collected beginning at 9:56 AM, after completion of the vertical profiling phase of the survey. During the subsequent twelve minutes, each station was re-occupied beginning with Station RW1. After auxiliary observations were collected at Station RW1, stations were sampled sequentially progressing toward the south. During that time, wind speed and air temperature remained relatively constant. A swell out of the northwest had a significant wave height of three-to-four feet. At 22°C, average air temperature was somewhat warmer than the 15.8°C sea surface temperature.

[21] Figure 9f, shown later in this report, includes a dark-green linear feature extending from the diffuser structure toward the north northwest. That feature is not apparent in the other property maps (Figure 9abcde) and is an artifact of the very slightly higher pH reported by the sensor as it neared equilibration while the CTD continued to traverse the two initial tow transects (D1 and D2). These two transects were nearly collinear (See the labeling in Figure 7), and their paths matched the shape of the dark-green pH anomalies in Figure 9f.

Table 4. Standard Meteorological and Oceanographic Observations

Station	Location[22]		Diffuser Distance	Time	Air	Cloud Cover	Wind Avg	Wind Dir (from)	Swell Ht/Dir	Secchi Depth
	Latitude	Longitude	(m)	(PDT)	(°C)	(%)	(kt)	(°T)	(ft/°T)	(m)
RW1	35° 23.254' N	120° 52.498' W	90.7	9:56:31	22.5	0%	5.6	270	3-4 NW	4.5
RW2	35° 23.231' N	120° 52.501' W	49.3	9:59:03	22.6	0%	7.1	260	3-4 NW	4.0
RW3	35° 23.208' N	120° 52.499' W	17.3	10:01:23	22.5	0%	6.6	270	3-4 NW	4.0
RW4	35° 23.188' N	120° 52.503' W	14.3	10:03:44	22.2	0%	5.8	250	3-4 NW	4.0
RW5	35° 23.168' N	120° 52.502' W	45.8	10:05:41	22.1	0%	3.8	280	3-4 NW	4.5
RW6	35° 23.148' N	120° 52.502' W	81.3	10:07:55	22.4	0%	4.3	260	3-4 NW	4.5

There was no evidence of floating particulates, oil sheens, or any discoloration of the sea surface associated with the presence of wastewater constituents. There was no other visual indication of the presence of the discharge plume at or beneath the sea surface during the survey. Ambient light penetration beneath the sea surface was limited by a dense population of planktonic organisms within the upper water column. During upwelling, nutrients carried upward into the euphotic zone are assimilated by phytoplankton, whose populations increase and, along with their associated zooplanktonic herbivores; their elevated densities reduce the transmittance of ambient light.

Because of the plankton-induced turbidity increase, the Secchi disk faded from view at a relatively shallow depth of 4 m as it was lowered through the upper water column at each station (Table 4). The measured Secchi depth indicates that an 8-m euphotic zone was present during the survey, and that ambient light only penetrated through the upper half of the water column and did not extend to the 9.5-m level where the mid-depth tow was conducted.

Of particular interest was the 0.5 m increase in Secchi depth at the two southernmost Stations RW5 and RW6. The increased water clarity within the upper water column at those stations was due to the entrainment of deeper clearer seawater within the rising effluent plume. As the plume extended into the naturally turbid shallow mixed layer, its increased water clarity became apparent, and resulted in slightly deeper Secchi depths (4.5 m instead of 4 m in Table 4). The increased water clarity within the plume was not detected in the Secchi depth measured at the southern ZID Station RW4 because the rising plume was still too deep to alter water clarity significantly within the upper 4 m of the water column, and thereby affect the visual determination of the disappearance of the Secchi disk.[23]

Increased Secchi depths notwithstanding, most of the plume remained submerged within the survey area and there was no obvious visual expression of the plume at the sea surface. Similarly, no evidence of floating particulates, oil sheens, or any discoloration of the sea surface was visually apparent during the survey that might be potentially related to the presence of wastewater constituents.

Communication with plant personnel and subsequent review of effluent discharge properties around the time of the survey, confirmed that the treatment process was performing well. The 0.813 million gallons of effluent discharged on 19 September had a temperature of 23°C and a pH of 7.3. An effluent sample collected on 20 September, the day after the survey, had a suspended-solids concentration of 30 mg/L and

[22] Locations are the vessel positions at the time the Secchi depths were measured. These depart from the CTD profile locations listed in Table 2 because they were collected after completion of the CTD profiling.

[23] The vertical extent of the plume is delineated by the green shaded salinity anomalies in Figures 8def shown later in this report. At Station RW4 (Figure 8d), the upper portion of the rising plume only started to reach the 4-m depth at the limit of the Secchi depth measurements. In contrast, by the time the plume had traveled south to Stations RW5 and RW6 (Figure 8ef), the presence of the plume became apparent throughout the shallowest portion of the water column, and its increased water clarity was reflected in the increased Secchi depths reported at those stations.

a biochemical oxygen demand (BOD) of 39 mg/L. The oil and grease concentration measured within effluent discharged on the day of survey was estimated to be 2.8 mg/L, but was too low to be reliably quantified.

Instrumental Observations

Data collected during vertical profiling were processed in accordance with standard procedures (SCCWRP 2002), and are collated at 0.5-m depth intervals in Table 5. Data collected during the September 2017 survey documented strongly stratified conditions within Estero Bay that were indicative of the onset of an unusually strong late-season coastal upwelling event (refer to the inset in Figure 6). As described previously, upwelling of varying intensity occurs most of the year along the central California coast, with the strongest upwelling winds beginning in March or April and extending through early summer. The intensity of upwelling tends to decline in late summer and into fall, although pulses of sustained northwesterly winds still occur. An intense upwelling event results in the rapid influx of dense, cold, saline water at depth and leads to a sharp thermocline, halocline, and pycnocline where temperature, salinity, and density change rapidly over a small vertical distance. Under these highly stratified conditions, isotherms crowd together to form a density interface, which inhibits the vertical exchange of nutrients and other water properties, and which traps the effluent plume at depth thereby reducing the initial dilution of the effluent plume.

If the upwelling winds are only of moderate strength, occur only briefly, or have not occurred recently; then vertical mixing slowly erodes the sharp contrast between the surface and deep watermasses, and stratification appears as a more gradual vertical change in seawater properties that can extend throughout the water column. That was not the case during the September 2017 survey when seawater properties within the vertically uniform surface mixed layer changed rapidly beneath the layer (Figure 8abc). The seawater properties continued to change rapidly with increasing depth until they achieved the ambient seawater conditions representative of the deep watermass that migrated shoreward along the seafloor during upwelling.

This vertical transition zone was compressed and transported upward by the rising effluent plume. The plume's influence was apparent during hydrocasts at Station RW4, RW5, and RW6 (Figure 8def). Specifically, the steadily changing vertical gradients in ambient seawater properties shown in Figure 8abc, were perceptibly altered by the presence of the rising plume. In Figure 8def, the presence of dilute but perceptible effluent constituents was delineated by marked salinity reductions shown by green shading. The plume's vertical compression of the ambient vertical thermal gradients is apparent from a comparison between the ambient vertical profiles measured at upcoast ZID Station RW3 (Figure 8c), and the plume-altered profiles at downcoast ZID Station RW4 (Figure 8d).

The thermocline at Station RW3 (red line in Figure 8c), for example, spanned a 5-m depth range from 7 m to approximately 12 m. In contrast, at Station RW4 (red line in Figure 8d), upward transport of the plume (green shading) shifted the thermocline upward in the water column and compressed its vertical extent to about 1 m. At that station, the majority of the temperature drop was largely confined to depths between 4 and 5 m. Weaker gradients extended to a depth of 8 m. The associated mixing and entrainment caused by the rising plume produced nearly uniform seawater properties throughout the deepest half of the water column. In contrast, ambient seawater exhibited obvious vertical changes at mid-depth before reaching the more-uniform properties of the 4-m thick seafloor watermass. Seafloor entrainment and upward transport of these deep seawater properties within the rising effluent plume was responsible for the surprisingly uniform conditions within the lower half of the water column at Station RW4.

Table 5. Vertical Profile Data Collected on 19 September 2017

Depth (m)	Temperature (°C)						Salinity (‰)					
	RW-1	RW-2	RW-3	RW-4	RW-5	RW-6	RW-1	RW-2	RW-3	RW-4	RW-5	RW-6
0.5	15.818	15.794	15.740	15.660	15.663		33.471	33.467	33.470	33.468	33.468	
1.0	15.788	15.788	15.733	15.652	15.656	15.610	33.469	33.469	33.469	33.467	33.467	33.465
1.5	15.777	15.781	15.726	15.626	15.635	15.599	33.469	33.469	33.468	33.464	33.466	33.465
2.0	15.778	15.764	15.703	15.640	15.602	15.577	33.470	33.468	33.468	33.467	33.463	33.463
2.5	15.756	15.736	15.675	15.598	15.564	15.527	33.467	33.467	33.467	33.462	33.461	33.460
3.0	15.741	15.700	15.647	15.559	15.531	15.460	33.467	33.465	33.465	33.461	33.460	33.458
3.5	15.732	15.686	15.625	15.563	15.484	15.332	33.467	33.465	33.464	33.463	33.456	33.452
4.0	15.726	15.681	15.618	15.429	15.462	15.184	33.467	33.465	33.464	33.452	33.458	33.447
4.5	15.719	15.671	15.609	15.155	15.396	15.092	33.466	33.464	33.463	33.447	33.458	33.446
5.0	15.717	15.664	15.588	14.599	15.140	15.071	33.466	33.464	33.462	33.372	33.441	33.450
5.5	15.716	15.658	15.570	14.571	15.020	15.032	33.466	33.464	33.461	33.424	33.447	33.447
6.0	15.715	15.653	15.550	14.447	14.972	14.940	33.466	33.464	33.460	33.411	33.447	33.434
6.5	15.710	15.637	15.535	14.435	14.909	14.748	33.466	33.462	33.460	33.428	33.444	33.415
7.0	15.690	15.611	15.461	14.291	14.760	14.608	33.464	33.460	33.456	33.404	33.421	33.407
7.5	15.634	15.571	15.262	14.105	14.635	14.402	33.460	33.458	33.442	33.359	33.419	33.382
8.0	15.550	15.438	15.185	13.961	14.522	14.326	33.455	33.448	33.450	33.345	33.410	33.386
8.5	15.474	15.280	15.101	13.949	14.454	14.280	33.453	33.445	33.449	33.369	33.409	33.389
9.0	15.330	15.192	15.060	13.953	14.289	14.282	33.445	33.445	33.450	33.387	33.385	33.393
9.5	15.198	15.147	14.939	13.970	14.240	14.284	33.442	33.448	33.451	33.391	33.391	33.397
10.0	15.081	15.144	14.515	13.971	14.129	14.289	33.444	33.451	33.436	33.391	33.377	33.410
10.5	14.942	14.983	14.395	13.953	14.070	14.301	33.445	33.451	33.453	33.392	33.376	33.432
11.0	14.715	14.638	14.289	13.936	14.034	14.301	33.442	33.428	33.453	33.394	33.387	33.452
11.5	14.465	14.448	14.212	13.904	14.019	14.231	33.444	33.447	33.456	33.395	33.421	33.460
12.0	14.327	14.365	14.149	13.914	14.015	14.117	33.450	33.457	33.462	33.395	33.429	33.452
12.5	14.219	14.235	14.010	13.896	13.993	14.095	33.454	33.452	33.459	33.405	33.458	33.457
13.0	14.105	14.169	13.948	13.878	13.956	13.996	33.454	33.458	33.464	33.419	33.466	33.446
13.5	14.030	14.077	13.917	13.895	13.930	13.974	33.460	33.461	33.467	33.435	33.469	33.461
14.0	13.931	13.962	13.887	13.901	13.866	13.974	33.459	33.462	33.468	33.454	33.467	33.463
14.5	13.856	13.880	13.855	13.884	13.861	13.930	33.462	33.463	33.469	33.465	33.469	33.466
15.0	13.821	13.847	13.847	13.875	13.839	13.912	33.465	33.467	33.471	33.474	33.470	33.468
15.5	13.807	13.820	13.848	13.860	13.805	13.869	33.468	33.468	33.472	33.472	33.472	33.469
16.0	13.803	13.817	13.853	13.850	13.751	13.781	33.470	33.471	33.474	33.473	33.472	33.471
16.5	13.805	13.818	13.857	13.818	13.742	13.751	33.480	33.480	33.475	33.473	33.475	33.479
17.0					13.746						33.480	

Table 5. Vertical Profile Data Collected on 19 September 2017 (continued)

Depth (m)	Density (σ_t)						pH					
	RW-1	RW-2	RW-3	RW-4	RW-5	RW-6	RW-1	RW-2	RW-3	RW-4	RW-5	RW-6
0.5	24.613	24.615	24.630	24.646	24.645		8.178	8.174	8.169	8.169	8.164	
1.0	24.618	24.618	24.630	24.647	24.646	24.655	8.178	8.175	8.170	8.166	8.162	8.166
1.5	24.620	24.620	24.631	24.651	24.650	24.657	8.177	8.174	8.171	8.167	8.164	8.164
2.0	24.621	24.623	24.636	24.650	24.655	24.660	8.177	8.175	8.171	8.166	8.165	8.165
2.5	24.624	24.628	24.641	24.655	24.662	24.669	8.178	8.176	8.170	8.168	8.165	8.162
3.0	24.627	24.635	24.646	24.663	24.669	24.682	8.179	8.173	8.171	8.167	8.165	8.156
3.5	24.629	24.638	24.650	24.664	24.676	24.706	8.179	8.175	8.171	8.165	8.163	8.151
4.0	24.630	24.639	24.652	24.685	24.682	24.735	8.181	8.175	8.171	8.161	8.163	8.139
4.5	24.631	24.641	24.654	24.741	24.697	24.754	8.182	8.176	8.172	8.151	8.159	8.122
5.0	24.631	24.642	24.657	24.803	24.739	24.762	8.183	8.177	8.172	8.126	8.151	8.115
5.5	24.631	24.643	24.661	24.850	24.770	24.768	8.184	8.175	8.172	8.096	8.135	8.110
6.0	24.632	24.644	24.664	24.866	24.781	24.778	8.184	8.176	8.168	8.078	8.113	8.105
6.5	24.633	24.647	24.667	24.881	24.792	24.805	8.185	8.174	8.168	8.058	8.101	8.096
7.0	24.636	24.650	24.681	24.893	24.806	24.829	8.185	8.172	8.164	8.045	8.092	8.085
7.5	24.646	24.658	24.714	24.898	24.832	24.853	8.187	8.172	8.155	8.035	8.085	8.064
8.0	24.660	24.680	24.737	24.916	24.849	24.872	8.182	8.170	8.138	8.017	8.066	8.049
8.5	24.676	24.712	24.754	24.938	24.862	24.884	8.177	8.156	8.121	8.003	8.058	8.042
9.0	24.701	24.732	24.764	24.950	24.879	24.887	8.168	8.137	8.111	8.000	8.043	8.038
9.5	24.728	24.744	24.791	24.950	24.894	24.889	8.149	8.129	8.104	8.000	8.037	8.035
10.0	24.755	24.747	24.870	24.950	24.906	24.899	8.136	8.127	8.096	8.001	8.026	8.032
10.5	24.786	24.781	24.909	24.954	24.917	24.913	8.125	8.116	8.072	8.000	8.016	8.033
11.0	24.832	24.838	24.932	24.959	24.934	24.928	8.112	8.097	8.053	7.999	8.007	8.033
11.5	24.887	24.893	24.950	24.967	24.963	24.949	8.093	8.087	8.042	7.996	8.007	8.036
12.0	24.921	24.918	24.968	24.965	24.970	24.967	8.067	8.079	8.034	7.995	8.009	8.033
12.5	24.947	24.942	24.995	24.976	24.997	24.975	8.046	8.055	8.029	7.995	8.011	8.028
13.0	24.971	24.960	25.011	24.991	25.011	24.987	8.038	8.044	8.021	7.993	8.011	8.016
13.5	24.991	24.982	25.020	25.000	25.019	25.003	8.029	8.034	8.015	7.993	8.008	8.009
14.0	25.011	25.006	25.027	25.013	25.031	25.005	8.020	8.024	8.011	7.994	7.999	8.008
14.5	25.028	25.024	25.035	25.025	25.033	25.016	8.014	8.016	8.006	7.997	7.998	8.006
15.0	25.038	25.034	25.037	25.034	25.038	25.022	8.008	8.010	8.002	7.998	7.995	8.002
15.5	25.043	25.041	25.038	25.036	25.047	25.031	8.002	8.004	8.000	7.997	7.991	7.999
16.0	25.046	25.043	25.038	25.038	25.058	25.051	7.996	7.997	7.997	7.997	7.989	7.992
16.5	25.046	25.043	25.038	25.045	25.062	25.051	7.995	7.998	7.994	7.992	7.985	7.989
17.0					25.062						7.984	

Table 5. Vertical Profile Data Collected on 19 September 2017 (continued)

Depth (m)	Dissolved Oxygen (mg/L)						Transmissivity (%)					
	RW-1	RW-2	RW-3	RW-4	RW-5	RW-6	RW-1	RW-2	RW-3	RW-4	RW-5	RW-6
0.5	8.427	8.439	8.331	8.350	8.310		82.447	81.420	83.044	80.737	83.129	
1.0	8.474	8.427	8.352	8.368	8.333	8.314	82.663	82.446	82.699	81.378	83.116	81.646
1.5	8.463	8.416	8.354	8.366	8.336	8.320	81.198	82.623	82.407	80.508	82.670	81.342
2.0	8.473	8.430	8.370	8.378	8.338	8.248	82.117	82.521	82.151	80.634	81.235	81.657
2.5	8.492	8.457	8.377	8.370	8.324	8.183	82.059	82.303	81.332	79.906	80.248	81.361
3.0	8.521	8.469	8.394	8.235	8.321	7.988	80.498	81.155	79.860	79.452	78.827	79.657
3.5	8.525	8.475	8.390	8.038	8.330	7.817	78.699	78.318	78.941	77.463	77.554	79.054
4.0	8.554	8.492	8.404	7.586	8.019	7.736	77.661	77.706	78.582	77.067	76.924	79.243
4.5	8.572	8.487	8.414	7.073	7.546	7.700	75.564	76.670	77.967	80.721	76.480	80.520
5.0	8.573	8.487	8.401	7.083	7.581	7.645	75.148	75.643	77.388	87.050	77.084	81.357
5.5	8.595	8.437	8.370	6.966	7.528	7.506	74.408	74.489	76.834	88.560	80.977	82.359
6.0	8.596	8.440	8.368	6.920	7.325	7.213	74.260	73.927	76.025	89.404	84.659	82.609
6.5	8.573	8.434	8.155	6.508	7.218	7.182	74.149	73.189	75.698	89.686	86.119	84.010
7.0	8.510	8.327	7.835	6.439	7.110	6.921	74.948	73.554	75.157	90.136	85.997	85.346
7.5	8.398	8.066	7.849	6.369	7.010	6.816	75.304	73.946	75.610	90.114	86.239	86.592
8.0	8.195	7.968	7.632	6.376	6.815	6.762	78.327	74.591	77.214	90.486	87.104	88.190
8.5	7.861	7.747	7.584	6.377	6.726	6.785	80.393	76.851	81.375	90.737	87.583	88.913
9.0	7.744	7.732	7.302	6.381	6.711	6.786	81.363	79.446	84.223	90.813	88.797	89.082
9.5	7.657	7.740	6.766	6.373	6.455	6.800	83.724	83.249	84.753	90.844	88.975	89.086
10.0	7.370	7.297	6.878	6.346	6.488	6.800	83.132	84.073	86.754	90.690	89.370	89.303
10.5	7.004	6.762	6.725	6.309	6.468	6.796	85.415	84.495	88.707	90.614	89.771	89.295
11.0	6.766	6.812	6.700	6.290	6.459	6.611	87.541	86.429	90.449	90.800	90.030	90.330
11.5	6.747	6.804	6.663	6.293	6.473	6.571	88.989	86.692	91.236	91.119	90.584	91.183
12.0	6.640	6.676	6.455	6.260	6.430	6.578	89.854	88.691	91.772	90.981	91.830	92.063
12.5	6.549	6.610	6.447	6.267	6.403	6.417	90.930	90.723	92.963	91.075	92.726	92.425
13.0	6.521	6.553	6.422	6.326	6.324	6.424	92.276	91.781	93.751	91.491	93.069	92.832
13.5	6.404	6.415	6.375	6.314	6.259	6.432	93.014	92.587	93.896	91.850	92.918	92.959
14.0	6.304	6.346	6.296	6.287	6.243	6.308	93.310	93.347	93.930	92.252	93.217	92.962
14.5	6.293	6.326	6.289	6.278	6.213	6.289	93.864	93.837	93.678	92.622	93.291	93.450
15.0	6.252	6.284	6.269	6.235	6.149	6.204	94.027	94.003	93.038	93.134	93.399	93.502
15.5	6.221	6.244	6.249	6.216	6.097	6.088	93.579	93.556	92.786	92.967	93.460	93.545
16.0	6.222	6.279	6.190	6.208	6.099	6.168	91.120	92.101	91.202	92.982	93.186	93.327
16.5	6.220	6.271	6.182	6.207	6.105	6.120	90.655	92.100	89.481	92.775	93.064	93.179
17.0					6.093						92.646	

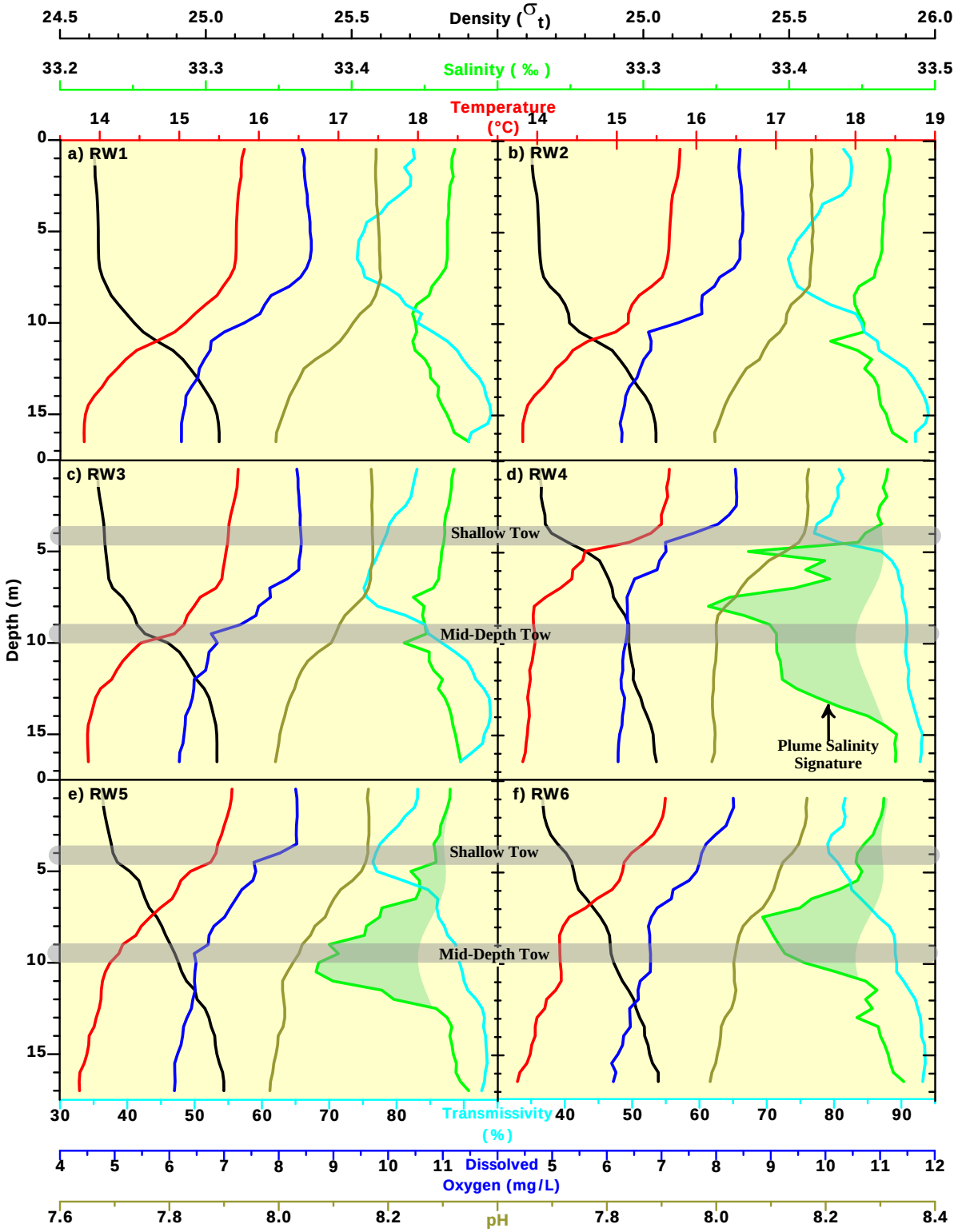

Figure 8. Vertical Profiles of Water-Quality Parameters

Plume-generated thermocline compression aside, the overall vertical structure within the survey area reflects a well-documented vertical transition from a shallow, locally generated watermass characteristics to a deep watermass created well offshore of the survey area. The warm, oxygen-rich conditions within the surface mixed layer were produced by local insolation, by atmospheric gas exchange, and by vertical mixing caused by surface wind and wave forces. The colder, saltier, nutrient-rich but oxygen-poor conditions within the deep watermass arose because they migrated shoreward along the seafloor as part of the upwelling process. This offshore watermass moved shoreward to replace nearshore surface waters that were driven offshore by Ekman transport from the prevailing northwesterly winds (Figure 5). The seawater properties of this deep watermass originated within the northward-flowing Davidson undercurrent that carried more saline and less oxygenated waters out of the Southern California Bight and northward along the central California coast.

Thus, intense upwelling in the days prior to, and during, the survey produced predicable changes in seawater properties within a vertical transition zone between the shallow and deep watermasses; namely, seawater properties exhibited steadily increasing or decreasing values with depth that were determined by well-established physicochemical processes (refer to Figure 8abc for profiles unaffected by the discharge). Specifically, temperature (red lines), DO (dark blue lines), pH (olive-colored lines) steadily decreased with increasing depth. These decreases were mirrored by a pycnocline, where density (black lines) steadily increased with depth. Transmissivity (light blue lines) also steadily increased with increasing depths beneath 7 m, until a 2.5-m-thick seafloor boundary layer associated with the deep watermass was encountered.

Meanwhile, within the shallow reaches of the water column, upwelling-enhanced primary productivity produced oxygen (increasing DO), consumed carbon dioxide (increasing pH), and increased phytoplankton density (decreasing transmissivity). In contrast, the lower temperature, DO, and pH of the seafloor watermass resulted from its origin deep offshore. Because it had not been in recent direct contact with the atmosphere, biotic respiration and decomposition had depleted its DO levels (dark blue lines). Additionally, at depth, these respiration and decomposition processes produced carbon dioxide (CO_2). In its dissolved state, the increased concentration of carbonic acid appears as a concomitant reduction in pH (olive-colored lines).

As expected from its higher density, the deep watermass migrated shoreward along the seafloor, which accounts for the uniformly low temperature, DO, and pH seen below 14 m (red, dark-blue, and gold lines in Figure 8abc). Additionally, seawater clarity was markedly higher within the deep watermass, as compared to that of the surface mixed layer (light-blue lines). However, the transmissivity profiles also exhibit some minor vertical structure within the two watermasses that produced localized extrema not apparent in the profiles of other seawater properties. Within the upper water column, the localized transmissivity minimum indicates that planktonic organisms were more concentrated near the bottom of the euphotic zone as compared to the sea surface.

Conversely, within the deep watermass, another process produced a much-smaller localized water-clarity maximum near 14.5 m. The slight 3.5% transmissivity reduction at the seafloor as compared to 2 m above the seafloor arose because of naturally occurring resuspension processes associated with boundary layer flow along the seafloor. The shoreward movement of the deep watermass generates increased turbulence and shear within a benthic nepheloid layer (BNL). These thin, transient, particle-rich layers form when lightweight flocs of detritus are resuspended by the turbulence generated from bottom currents. BNLs are a widespread phenomenon on continental shelves (Kuehl et al. 1996) and have been regularly documented in past surveys conducted within Estero Bay.

In addition to the aforementioned influence of natural processes on the vertical trends in seawater properties, the downcasts at Stations RW4 through RW6 (Figure 8cde) encountered the effluent plume at various depth levels as the plume rose within the water column and was transported southward. As discussed previously, the plume's presence perceptibly altered the vertical distribution of ambient seawater properties. Not surprisingly, the most pronounced plume effect was apparent in the profiles at Station RW4 (Figure 8d), which was located immediately downstream (down current) of the diffuser structure. At that ZID station, the largest salinity declines spanned a remarkably wide depth range from 5 m to 14 m (green shading on the salinity profile). As described previously, below 8 m, where the salinity signature was strongest, other seawater properties were nearly vertically uniform and in stark contrast to the steadily changing properties in ambient seawater seen at Station RW3 (Compare the red, dark-blue, gold, and light-blue lines in Figure 8c with those of Figure 8d).

The depth range of vertically uniform seawater properties at Station RW4 (Figure 8d) was larger than at the other two stations affected by the discharge (Figure 8ef). Notably, it corresponds to differences in the vertical extent of the plume shown by the green shading. As described previously, the water-property uniformity within the plume reflects the presence of ambient seawater that was entrained near the seafloor. The cold clear seawater mixed rapidly with effluent shortly after discharge, and the diluted effluent took on the characteristics of the surrounding ambient seawater. These characteristics were then carried upward in the water column by buoyant effluent plume. As the plume initially moved rapidly into the upper water column, it compressed the gradual vertical gradients seen at stations unaffected by the plume (northern Stations RW1, RW2, and RW3 in Figure 8abc), into a very sharp vertical transition zone near 4 m (red, dark-blue, and gold lines in Figure 8d). As the plume migrated farther south to Stations RW5 and RW6, the plume's vertical extent began to collapse around its equilibrium (trapping) depth near 8 m as it began to spread laterally (light green shading in Figures 8ef).

The profile data demonstrate that vertical stratification within the water column at the time of the survey was of sufficient strength to trap the effluent plume beneath the sea surface. During most surveys, when the water column is less stratified, the buoyant plume rises all the way to the sea surface where it spreads laterally. On those occasions, the location of surfacing plume is often visually apparent as a reduction in capillary waves over a limited area within the ZID. However, during stratified conditions, the plume can become trapped at depth, which curtails the additional buoyant mixing normally experienced during the plume's ascent through the entire water column.

Although the vertical profile data at Stations RW5 and RW6 demonstrate that the subsurface plume had become trapped at a depth near 8 m (light green shading in the salinity profiles of Figure 8ef), the September 2017 survey data also provide unusual insight into the dynamics of the plume trapping process. Specifically, the smaller isolated salinity reduction near 5 m at Station RW4 (Figure 8d) demonstrates that the momentum of the rising effluent plume initially carried it beyond its buoyant-equilibrium depth and closer to the sea surface. Subsequently, as the plume's upward momentum dissipated, gravitational forces began to dominate the dilute effluent-seawater mixture, and the plume began to descend as it was transported farther south by the prevailing current. These vertical oscillations about the buoyancy equilibrium depth are a well-described phenomenon in atmospheric and oceanographic dynamics. In fact, the buoyancy oscillation frequency can be determined analytically from the strength of water-column stratification.[24]

[24] The Väisälä-Brunt frequency, or buoyancy frequency, is the frequency at which a vertically displaced water parcel will oscillate within a statically stable environment. Because of its direct relation to stability, it is often cited as an alternative measure of the degree of water-column stratification.

The oscillatory motion of the effluent plume during its southward migration was also captured by the mid-depth tow survey (Figure 9b), and to a lesser extent during the shallow tow (Figure 10b). The mid-depth tow was conducted at a depth (9.5 m) that was somewhat below the 8 m plume trapping depth (bottom thick shaded horizontal line spanning Figure 8f). Consequently, the mid-depth tow captured the plume's vertical oscillations about its buoyant equilibrium depth during its southward migration. At Station RW4, the lowest salinity was slightly shallower than the tow depth (lower shaded horizontal line Figure 8d). Farther south, the vertical cast at Station RW5 delineated the plume centroid beneath the mid-depth tow (Figure 8e), while at Station RW6, the plume was centered at a depth above the tow depth Figure 8f). These vertical excursions in the plume were captured by the patches of reduced salinity that can be seen extending due south of the diffuser structure in Figure 9b.

In contrast, the 4.2-m shallow tow was conducted well above the trapping depth. As a result, the shallow tow only captured a significant plume signature within a limited area of the ZID (red shading in Figure 10b) where its upward momentum briefly caused it to overshoot its buoyancy equilibrium level. Its positive buoyancy at that location was confirmed by plume density measurements that were higher than the surrounding seawater (note the reversed density scale in Figure 10c). In contrast, the near-neutral plume density close to the trapping depth was reflected by the general absence of density anomalies coincident with the plume signature during the mid-depth tow (Figure 9c).

Additionally, during both tows, anomalies in seawater properties were delineated over wide areas at locations that did not coincide with the salinity anomalies. Salinity anomalies that definitively delineate the presence of dilute wastewater constituents were largely restricted to a region near the ZID, and in locations directly south (Figures 9b and 10b). In contrast, a large pool seawater with anomalous properties was delineated well west of the discharge during the shallow tow (Figure 10acdef). This pool exhibited properties consistent with the upward transport of ambient seawater, namely, slightly lower temperature, DO, and pH (Figure 10aef), and increased density and transmissivity (reversed scale in Figure 10cd). Although the origin of this pool of anomalous seawater properties near the western margin of the survey area is indeterminate, the pool was clearly not caused by local alterations due to the presence of dilute wastewater constituents. Not only were salinity decreases absent, but the warmer, turbid, buoyant wastewater constituents would be expected to increase temperature, and decrease density and transmissivity; changes that were opposite of that observed in the anomalous shallow pool west of the discharge point.

Two possibilities could explain the presence of this western pool of anomalies. First, the shallow anomalies could have been produced by plume entrainment at some time prior to the survey, when a flow reversal caused anomalies produced prior to the survey to be reintroduced into the survey area. Flow changes prior to the survey may have been associated with the tide reversal that occurred immediately prior to the survey (Figure 4). Because entrainment anomalies are generated by the physical movement of ambient seawater, and not plume-dilution processes, they can be particularly long lived, and can remain apparent long after the wastewater constituents have dispersed far beyond recognition.

The second possible explanation for the odd distribution of anomalies is most apparent in the mid-depth tow data (Figure 9acdef). None of those anomalies coincided spatially with the salinity anomalies (Figure 9b), and often they were not spatially consistent among the various seawater properties. Instead, they appear to be collinear the tracklines (compare the distribution of anomalies in Figure 8acdef with the tracklines in Figure 8b). As described in Footnote 21 on Page 13, the elongated section of increased pH seen extending to the north northwest of the diffuser structure (thick dark-green line in Figure 9f) was an artifact of very slight ongoing equilibration of the pH sensor during the first two transects (D1 and D2).

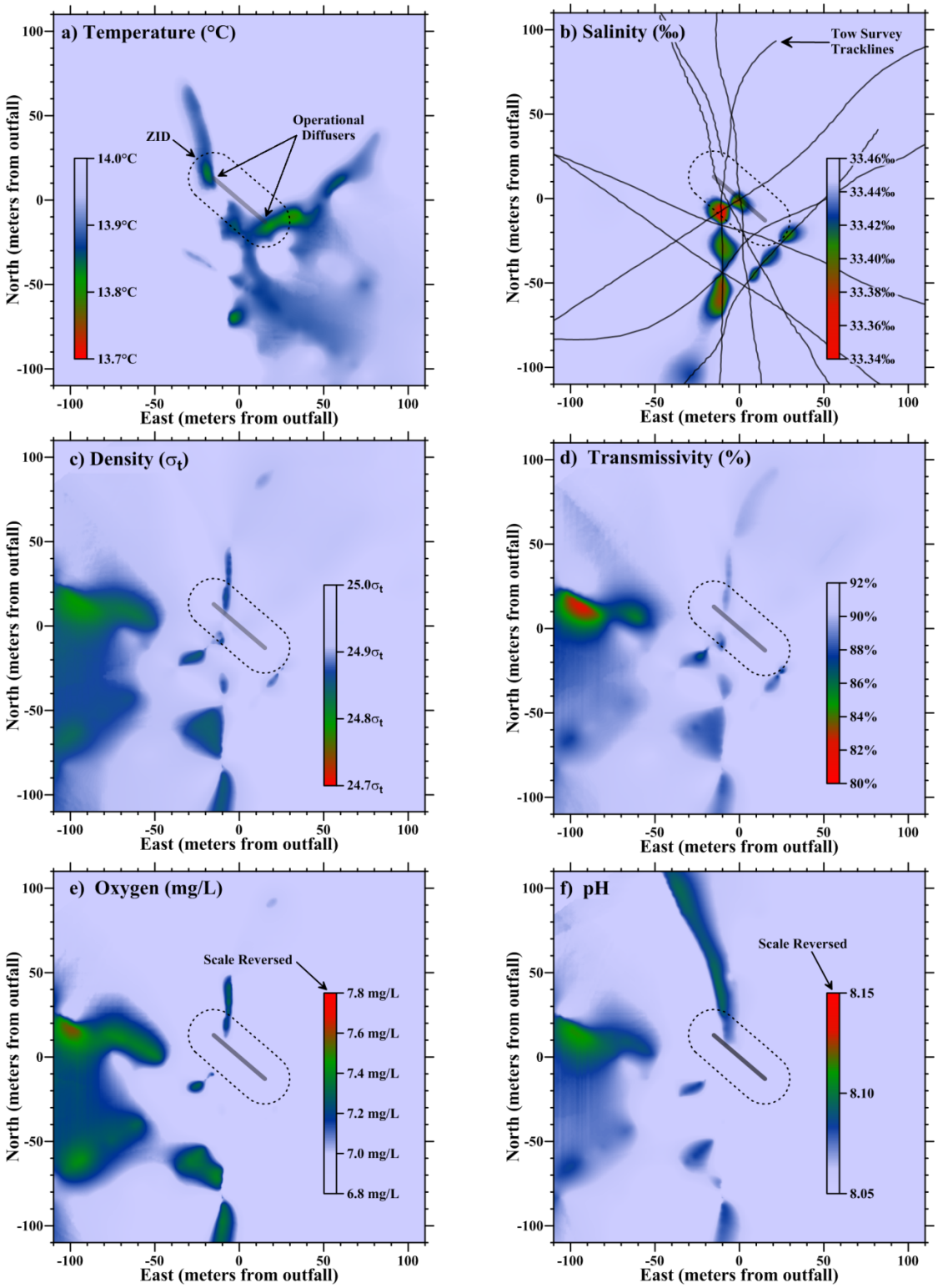

Figure 9. Horizontal Distribution of Mid-Depth Water-Quality Parameters 9.5 m below the Sea Surface

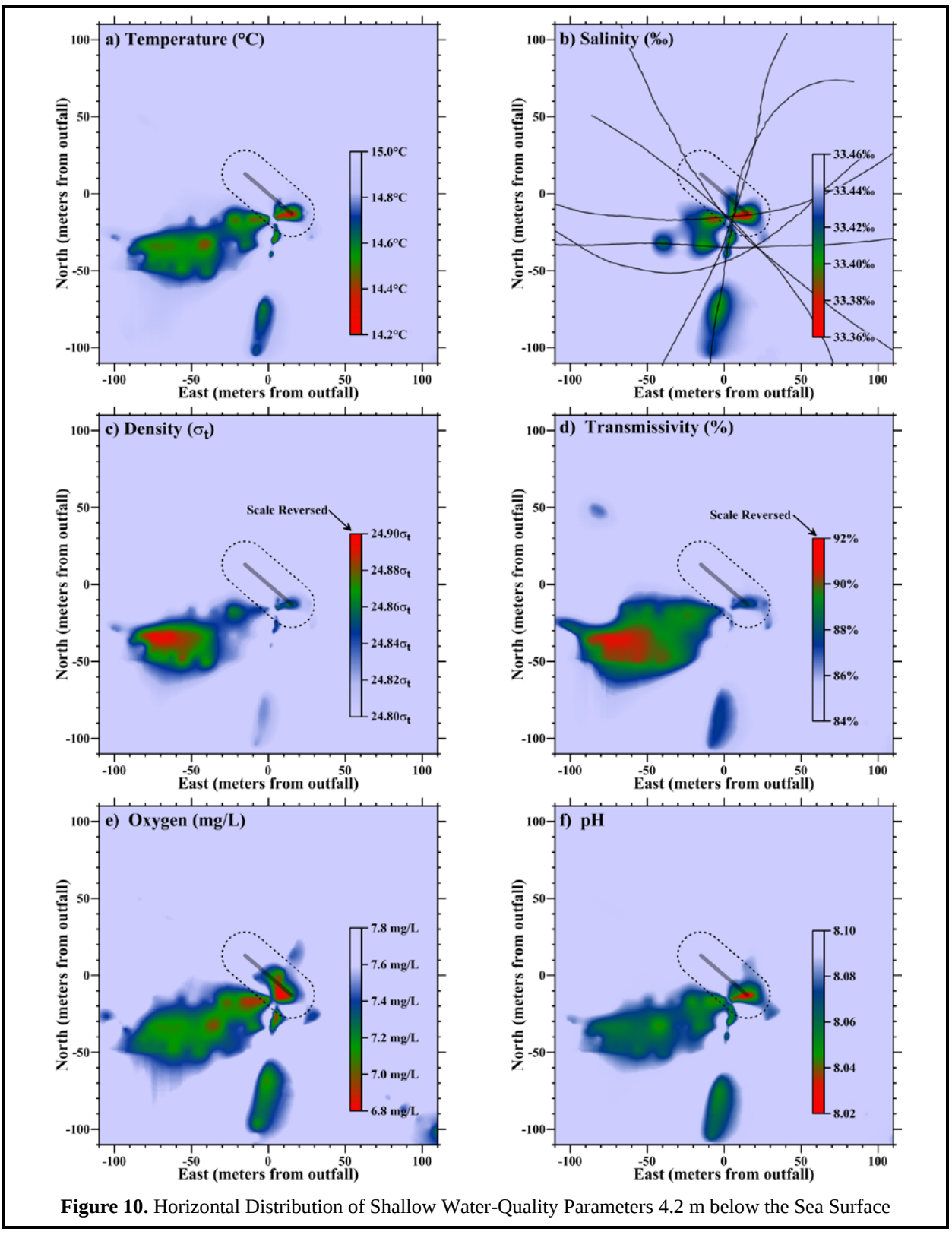

Figure 10. Horizontal Distribution of Shallow Water-Quality Parameters 4.2 m below the Sea Surface

Similarly, the other anomalies may have been artificially generated by slight changes in tow depth that produced lateral anomalies when different portions of the sharp vertical gradients were encountered. As apparent from the narrow scale ranges in the horizontal tow maps, these horizontal anomalies had very small amplitudes. They could have been easily generated by a vertical fluctuation of less than a meter in tow depth.

Regardless, the series of seawater anomalies located immediately south of the diffuser structure were clearly related to the presence of wastewater constituents. Their locations were directly aligned the southward oceanic current flow measured by the drifter at the time of survey, and they coincided with the salinity reductions delineated in Figures 9b and 10b. In particular, the elongated green and dark blue anomaly located at the southern extreme of the shallow tow area (Figure 10acdef) coincided with a slight reduction in salinity (Figure 10b). Although the reduced salinity suggests the presence of very dilute wastewater constituents, those constituents were not responsible for generating the anomalies seen in other seawater properties. Although discharge-related, the excursions seen in temperature, transmissivity, DO, and pH during the survey were caused by the entrainment and upward transport of ambient seawater. It is important to distinguish plume signatures that are caused by the presence of effluent constituents, exemplified by marked reductions in salinity, from those caused by the upward transport of ambient seawater, embodied by the lateral anomalies in all the other seawater properties.

Expanding on the physical process of entrainment, close to the seafloor, intense mixing is driven by the momentum of the effluent's ejection from the individual diffuser ports. Subsequent turbulent mixing caused by the plume's ascent through the water column is less intense, and as a result, the dilute effluent plume tends to retain the ambient seawater properties it acquired at the seafloor. During the September 2017 survey, these deep seawater properties became apparent as a signature of the buoyant effluent plume when they were juxtaposed against the ambient seawater characteristics in the mid and upper water column. These entrainment-generated anomalies are only apparent, however, when the water column is sufficiently stratified to cause a perceptible contrast between the shallow and deep ambient seawater properties.

As described previously, the legacies of entrainment anomalies can be particularly long-lived, remaining apparent within the water column well after completion of the initial dilution process. Anomalies, such as those captured on the southern limit of the survey area during the shallow tow, provide useful tracers of the diffuse effluent plume during and after the completion of the initial dilution process. However, such anomalies are irrelevant to the receiving-water compliance assessment because the permit restricts attention to water-quality changes caused solely by the presence of wastewater constituents rather than by a simple relocation of ambient seawater.

Outfall Performance

The efficacy of the outfall can be evaluated through a comparison of dilution levels measured at the time of the September 2017 survey, and dilutions anticipated from modeling studies that were codified in the discharge permit through limits imposed on effluent constituents. Specifically, the critical initial dilution applicable to the MBCSD outfall was conservatively estimated to be 133:1 (Tetra Tech 1992). That is, dispersion modeling estimated that, at the conclusion of the minimum expected initial mixing, 133 parts of ambient seawater would have mixed with each part of wastewater.

The 133:1 dilution estimate was based on worst-case modeling under highly stratified conditions, where trapping of the plume below a strong thermocline would curtail the additional buoyant mixing normally experienced during the plume's ascent through the entire water column. Additionally, the modeling assumed quiescent oceanic flow conditions, thereby restricting initial mixing processes to the ZID. Under

those conditions, the modeling predicted that a 133:1 dilution would be achieved after the plume rose only 9 m from the seafloor, whereupon it would become trapped, ceasing to ascend farther in the water column. At that point, the plume would spread laterally with dilution occurring at a much-reduced rate. A 9-m ascent at the MBCSD outfall translates into a trapping depth that is 6.4 m below the sea surface. As described below, however, the lowest dilution levels observed during the September 2017 survey were much higher than the 133:1 predicted by the modeling, even though they were measured within the ZID, at greater depth, and well before the completion of the initial dilution process.

The conservative nature of the critical initial dilution determined from the modeling is an important consideration because it was used to specify permit limitations on chemical concentrations within wastewater discharged from the treatment plant. These end-of-pipe effluent limitations were back calculated from the receiving-water objectives in the COP (SWRCB 2005) using the projected 133-fold dilution determined from the modeling. Application of a higher critical dilution would relax the stringent end-of-pipe effluent limitations thought necessary to meet COP objectives after initial dilution is complete.

End-of-pipe limitations on contaminant concentrations within discharged wastewater were based on the definition of dilution (Fischer et al. 1979). From the mass-balance of a conservative tracer, the concentration of a particular chemical constituent within effluent before discharge (C_e) can be determined from Equation 1.

$$C_e \equiv C_o + D\left(C_o - C_s\right) \qquad \text{Equation 1}$$

where: C_e = the concentration of a constituent in the effluent,
C_o = the concentration of the constituent in the ocean after dilution by D (i.e., the COP receiving-water objective),
D = the dilution expressed as the volumetric ratio of seawater mixed with effluent, and
C_s = the background concentration of the constituent in ambient seawater.

By rearranging Equation 1, the actual dilution achieved by the outfall can be determined from measured seawater anomalies. This measured dilution can then be compared with the critical dilution factor determined from modeling. Salinity is an especially useful tracer because it directly reflects the magnitude of ongoing dilution. The regions of slightly lower salinity apparent south of the outfall in both tow-survey maps (Figures 9b and 10b), and in the vertical profiles measured at the southernmost stations (Figure 8def) were induced by the presence of dilute wastewater. These salinity anomalies document mixing processes within the effluent plume shortly after discharge, and as it rose through the water column and spread laterally near its trapping depth.

The amplitudes of these salinity anomalies quantify the magnitude of wastewater dilution at the various stages of the initial mixing process. By rearranging Equation 1, the dilution ratio (D) can be computed from the salinity anomaly ($A = C_o - C_s$) as:

$$D \equiv \frac{(C_e - C_o)}{\left(C_o - C_s\right)} \propto A^{-1} \qquad \text{Equation 2}$$

The salinity concentration within MBCSD effluent (C_e)[25] is small compared to that of the receiving seawater and, after dilution by more than 133 fold, the salinity of the effluent-seawater mixture is close to ambient salinity. Consequently, to a close approximation, dilution levels are inversely proportional to the amplitude of the salinity anomaly. Thus, a lower effluent dilution at a given location within the effluent plume is directly mirrored by a larger reduction in the measured salinity relative to that of the surrounding seawater.

Among the 11,615 CTD measurements collected during the September 2017 survey, the greatest reduction in salinity (-0.131‰) was recorded during the ninth transect of the mid-depth tow survey when a salinity of 33.445‰ was encountered only 14.5 m from the middle of the diffuser structure at a depth of 8.1 m (red shading in Figure 9b). From Equation 2, this salinity anomaly corresponds to a dilution of 258 fold (small patch of red along the southwest ZID boundary in Figure 11). This level of dilution was similar to the 302-fold dilution associated with the lowest salinity measured nearby during vertical profiling. It was measured at a depth of 8 m at Station RW4 (green profile in Figure 8d), which was very close to the location of the lowest dilution measured during mid-depth tow.

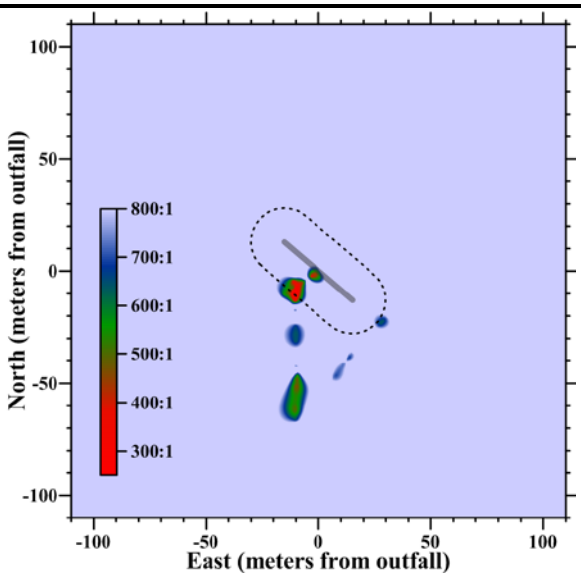

Figure 11. Mid-Depth Plume Dilution Computed from Salinity Anomalies in Figure 9b

The plume continued to mix as it traveled south and oscillated vertically. As a result, progressively lower dilutions were encountered during the tow surveys, as well as during vertical profiling. The other pool of perceptibly lower salinity encountered during the mid-depth tow was located 60 m south of the discharge point and contained effluent that had been diluted at least 437 fold (southernmost patch of green shading in Figure 11). Similar dilution levels were captured at the southernmost Stations RW5 and RW6 in conjunction with the minimum salinities measured near the level of the mid-depth tow (green shading in Figure 8ef).

The shallow tow also captured pools of dilute effluent constituents as the plume temporarily migrated upward during its transport south (Figure 12). The lowest dilutions of 307 fold were encountered over the southeast end of the diffuser structure. Dilutions exceeding 510 fold were encountered in a separate pool 75-m south of the discharge point.

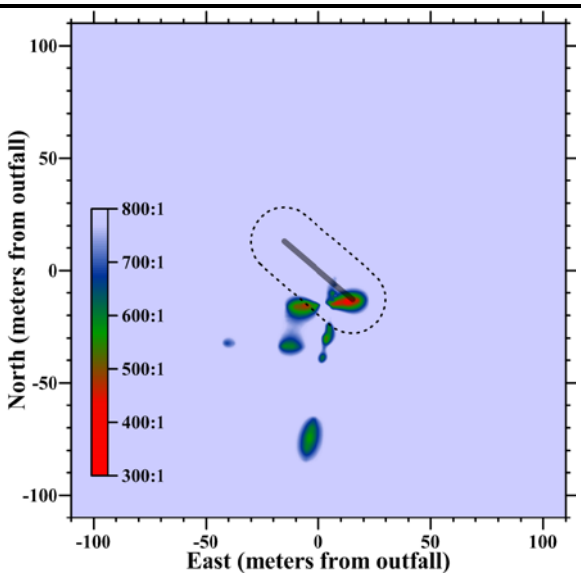

Figure 12. Shallow Plume Dilution Computed from Salinity Anomalies in Figure 10b

[25] Wastewater samples have an average salinity of 0.995‰.

These measurements confirm that the plume was continuing to experience rapid initial dilution well beyond the ZID. The rapid ongoing dilution resulted from large vertical oscillations about its 8-m trapping depth. By the time the plume reached the southernmost portions of the survey area, the damped vertical oscillations had largely dissipated and the plume had settled near its equilibrium level. Thus, at the completion of the initial dilution process, wastewater constituents had been diluted at least 437 fold.

Overall, the dilution computations show that, during the September 2017 survey, the outfall was performing better than designed and was rapidly entraining seawater shortly after discharge. This resulted in dilution levels exceeding 248 fold only 14.5 m from the diffuser structure and long before the initial mixing process was complete. Although this dilution level was measured 1.7 m deeper than the trapping depth assumed in the worst-case modeling study, the plume had already achieved dilution levels 86% higher than predicted. As the plume was transported rapidly to the south, vertical buoyancy-inducted oscillations further increased the dilution to 437 fold as the initial mixing process was nearing completion. At that point, effluent dilution was more than triple the 133:1 critical initial dilution used to establish end-of-pipe permit limitations on contaminant concentrations within wastewater discharged from the MBCSD treatment plant. This demonstrates that, during the September 2017 survey, the COP receiving-water objectives were being easily met by the limits on chemical concentrations within discharged wastewater that are promulgated by the NPDES discharge permit issued to the MBCSD.

COMPLIANCE

This section evaluates compliance with the water-quality limitations listed in the NPDES permit (Table 6). The limits themselves are based on criteria in the COP, the Central Coast Basin Plan, and other state and federal policies that were designed to protect marine life and beneficial uses of ocean waters. Because the limits only pertain to changes in water properties that are caused by the presence of wastewater constituents beyond the ZID, instrumental measurements undergo a series of screening procedures prior to numeric comparison with the permit thresholds. Specifically, the quantitative analyses described in this section focus on water-property excursions caused by the presence of wastewater constituents beyond the ZID, whose amplitudes can be reliably discerned against the backdrop of ambient fluctuations. A detailed understanding of ambient seawater properties, and their natural variability within the region surrounding the outfall, is therefore an integral part of the compliance evaluation presented in this section.

Table 6. Permit Provisions Addressed by the Offshore Receiving-Water Surveys

Limit #	Limit
P1	Floating particles or oil and grease to be visible on the ocean surface
P2	Aesthetically undesirable discoloration of the ocean surface
P3	Temperature of the receiving water to adversely affect beneficial uses
P4	Significant reduction in the transmittance of natural light at any point outside the ZID
P5	The DO concentration outside the zone of initial dilution to fall below 5.0 mg/L or to be depressed more than 10% from that which occurs naturally
P6	The pH outside the zone of initial dilution to be depressed below 7.0, raised above 8.3, or changed more than 0.2 units from that which occurs naturally

The results of the analyses performed on the September 2017 data demonstrate that the MBCSD discharge complied with the NPDES discharge permit. Moreover, although observations within the ZID are not subject to compliance evaluations, they met the prescribed limits because actual dilution levels routinely exceeded the conservative design specifications assumed in the discharge permit. Thus, the quantitative evaluation described in this section documents an outfall and treatment process that was performing at a high level during the September 2017 survey.

Permit Provisions

The offshore receiving-water surveys are designed to assess compliance with objectives dealing with undesirable alterations to six physical and chemical characteristics of seawater. Specifically, the permit states that wastewater constituents within the discharge shall not cause the limits listed in Table 6 to be exceeded.

The first two receiving-water limits, P1 and P2, rely on qualitative visual observations for compliance evaluation. Compliance was demonstrated during the September 2017 survey through visual inspection of the sea surface that documented an absence of floating wastewater materials, oil, grease, and discoloration of the sea surface.

Compliance with the remaining four receiving-water limitations was quantitatively evaluated through a comparison between instrumental measurements and numerical limits listed in the NPDES permit. For example, in P5 and P6, the fixed numeric limits on absolute values of DO (>5 mg/L) and pH (7.0 to 8.3) can be directly compared with field measurements within the dilute wastewater plume beyond the ZID. However, both P5 and P6 also contain narrative limits, which originate within the COP, and define unacceptable water-quality impacts in terms of "*significant*" excursions beyond those that occur "*naturally*." Quantitative evaluation of these limits requires a further comparison of field measurements with numerical thresholds that reflect the natural variation in temperature, transmissivity, DO, and pH within the receiving waters surrounding the outfall.

As described in prior sections, natural variation in seawater properties can result from a variety of oceanographic processes. These processes establish the range in ambient seawater properties caused by natural spatial variation within the survey region at a given time (e.g., vertical stratification), and by temporal variations caused by seasonal and interannual influences (e.g., El Niño and La Niña). Of particular interest are upwelling and downwelling processes that not only determine average properties at a given time, but also the degree of water-column stratification, or spatial variability, present during any given survey.

Screening of Measurements

Evaluating whether any of the 11,615 CTD measurements collected during the September 2017 survey exceeded a permit limit can be a complex process. For example, although apparently significant excursions in an individual seawater property may be related to the presence of wastewater constituents, they may also result from instrumental errors, natural processes, entrainment of ambient bottom water in the rising effluent plume, statistical uncertainty, ongoing initial mixing within and beyond the ZID, or other anthropogenic influences (e.g., dredging discharges or oil spills).

Because of this complexity, measurements were first screened to determine whether numerical limits on individual seawater properties even apply (Table 7). The screening procedure sequentially applies three questions to restrict attention to: 1) the oceanic area where permit provisions pertain; 2) changes due to the presence of wastewater particulates; and 3) changes large enough to be reliably detected against the backdrop of natural variation. The measurements that remain after completing the screening process can then be compared with Basin-Plan numerical limits and COP allowances.

The subsection following this one provides additional lines-of-evidence that demonstrate compliance with numerical permit limits independent of the screening process. The rationale for identifying observations suitable for further compliance analysis is presented in the following descriptions of the three screening steps.

Table 7. Receiving-Water Measurements Screened for Compliance Evaluation

Topic Addressed	Screening Question	Answer No	Answer Yes[26]	*Parameter*
Location	1. Was the measurement collected beyond the 15.2-m ZID boundary where modeling assumes that initial dilution is complete?	*1,133*	*10,482*	All
Wastewater Constituents	2. Did the beyond-ZID measurement coincide with a quantifiable salinity anomaly (≤550:1 dilution level) indicating the presence of detectable wastewater constituents?	*10,352*	*130*	All
Natural Variation	3. Did seawater properties associated with the wastewater measurements depart significantly from the expected range in ambient seawater properties at the time of the survey?	*130*	*0*	Temperature
		130	*0*	Transmissivity
		130	*0*	DO
		130	*0*	pH

1. Measurement Location: The COP states that compliance with its receiving-water objectives "*shall be determined from samples collected at stations representative of the area within the waste field where initial dilution is completed.*" Initial dilution includes the mixing that occurs from the turbulence associated with both the ejection jet, and the buoyant plume's subsequent ascent through the water column.

Although currents often transport the plume well beyond the ZID before the initial dilution process is complete, the COP states that dilution estimates shall be based on "*the assumption that no currents, of sufficient strength to influence the initial dilution process, flow across the discharge structure.*" Because of this, the regulatory mixing distance, which is equal to the 15.2-m water depth of the discharge, provides a conservative boundary to screen receiving-water data for subsequent compliance evaluation. Application of this initial screening question to the September 2017 dataset eliminated 1,133 of the original 11,615 receiving-water observations from further consideration because they were collected within the ZID (Table 7, Question 1). The remaining 10,482 observations were carried forward in the screening analysis.

2. Presence of Wastewater Constituents: The MBCSD discharge permit restricts application of the numerical receiving-water limits to excursions caused by the presence of wastewater constituents. This confines the compliance analysis to changes caused "*as the result of the discharge of waste,*" as specified in the COP, rather than anomalies that arise from the upward movement of ambient seawater entrained within the buoyant effluent plume. Analyses conducted on quarterly receiving-water surveys over the last decade have demonstrated that the direct influence of dilute wastewater is almost never observed in any seawater property other than salinity, except very close (<1 m) to a diffuser port and within its ejection jet.

In fact, negative salinity anomalies are the only consistent indicator of the presence of wastewater constituents within receiving waters. Wastewater salinity is negligible compared to that of the receiving seawater, so the presence of a distinct salinity minimum provides *de facto* evidence of the presence of wastewater constituents. Because of the large contrast between the nearly fresh wastewater and the salty receiving water, salinity provides a powerful tracer of dilute wastewater that is unrivaled by other seawater properties. Other properties do not exhibit such a large contrast and, as such, their wastewater signatures dissipate rapidly upon discharge with very little mixing. Wastewater's lack of salinity, however, provides a definitive tracer that allows the presence of effluent constituents to be identified even

[26] Number of remaining CTD observations of potential compliance interest based on sequential application of each successive screening question

after dilution many times greater than the 133-fold critical initial dilution assumed in the discharge permit.

As described in the previous section, wastewater-induced reductions in salinity can be used to determine the amount of dilution achieved by initial mixing. Based on statistical analyses of the natural variability in salinity readings measured near the outfall over a five-year period between 2004 and 2008, the smallest reduction in salinity that can be reliability detected within receiving waters is 0.062‰. This represents a dilution level of 542 fold in Equation 2. Salinity reductions that are smaller than 0.062‰ cannot be reliably discerned against the backdrop of natural variation, and would not result in discernible changes in other seawater properties. Eliminating those measurements from further evaluation restricts attention to excursions in temperature, light transmittance, DO, and pH that are potentially related to the presence of wastewater constituents.

As discussed previously, the greatest salinity reductions observed during the September 2017 survey were recorded immediately southwest of the outfall during the mid-depth tow survey. Because of the strong oceanic flow, the submerged plume was carried well beyond the ZID as it experienced vertical buoyancy-induced oscillations before the initial dilution process was complete. As a result, an unusually large number of quantifiable salinity reductions were measured well south of the ZID boundary. Even though these 130 salinity anomalies were clearly measured prior to completion of the initial dilution process, they were outside the ZID and reliably associated with the presence of wastewater constituents (Table 7). The remaining 10,352 salinity measurements collected beyond the ZID during the September 2017 survey did not have salinity reductions that were larger than the 0.062‰ plume-detection threshold, and therefore corresponded to dilutions greater than 550:1.

3. Natural Variation: An integral part of the compliance analysis is determining whether a particular anomalous measurement resulted from the presence of wastewater constituents, or whether it simply became apparent because ambient seawater was relocated (upward) by the plume. If the measurement does not significantly depart from the natural range in ambient seawater properties at the time of the survey, then it is inappropriate to ascribe the departure to the presence of wastewater constituents. Thus, quantifying the natural variability around the outfall at the time of the survey is necessary for determining whether a particular observation warrants comparison with the numeric permit limits.

A statistical analysis of receiving-water data collected around the outfall was used to establish the range in natural conditions surrounding the outfall (first three data columns of Table 8 on the following page). These ambient-variability ranges were used to identify significant departures from natural conditions that could be indicative of adverse discharge-related effects on water quality. The same five-year database used to establish the within-survey salinity variation discussed previously, was also used to establish one-sided 95% confidence bounds on transmissivity (-10.2%), temperature (+0.82°C), DO (-1.38 mg/L), and pH (± 0.094). These were combined with 95th percentiles determined from the September 2017 ambient seawater data, to establish time-specific natural-variability thresholds in a manner analogous to COP Appendix VI. The percentiles were determined from September-2017 vertical profile data collected largely at Stations RW1, RW2, and RW3, and excluded all measurements potentially affected by the discharge at other stations.

Temperature, transmissivity, pH, and DO concentrations associated with the 130 remaining measurements of potential compliance interest were all well within their respective ranges of natural variability (Table 7, Question 3). As such, the screening process unequivocally eliminated all of the measurements collected during the September 2017 survey from further consideration in the compliance analysis. In fact, all of the documented excursions in these properties were the result of physical processes unrelated to the presence of wastewater constituents, namely, entrainment of near-bottom seawater within the rising effluent plume.

Table 8. Compliance Thresholds

Water Quality Property	95% Confidence Bound[27]	95th Percentile[28,29]	Natural Variability Threshold[30]	COP Allowance[31]	Basin Plan Limit[32]	Extremum[33]
Temperature (ºC)	0.82	15.76	>16.58	>18.78	—	≤15.82
Transmissivity (%)	-10.2	74.6	<64.4	—	—	≥73.2
DO (mg/L)	-1.38	6.17	<4.79	<4.31	<5.00	≥6.09
pH (minimum)	-0.094	7.994	<7.900	<7.700	<7.000	≥7.982
pH (maximum)	0.094	8.182	>8.276	>8.476	>8.300	≤8.187

As discussed previously, anomalies in seawater properties clearly delineated the plume, but those entrainment-generated excursions were not caused by the presence of wastewater constituents. During periods when the water column is even slightly stratified, ambient seawater properties near the seafloor differ from those within the rest of the water column, and their juxtaposition within the rising effluent plume appears as lateral anomalies within the upper water column. Regardless, if the presence of wastewater particulates had contributed to the observed decreases in DO, pH and transmissivity within the upper water column, their influence would still have been well within the natural range of the ambient seawater properties at the time of the survey. Consequently, their influence on water quality would not be considered environmentally significant.

Other Lines of Evidence

Several additional lines of evidence further support the conclusion that all the CTD measurements collected during the September 2017 survey complied with the quantitative permit limits P3 through P6 in Table 6. In combination, these lines of evidence provide the "best explanation" of the origin and significance of individual measurements using abductive inference (Suter 2007). This process, which has been used to implement sediment-quality guidelines for California estuaries (SWRCB 2009), emphasizes a pattern of reasoning that accounts for both discrepancies and concurrences among multiple lines of evidence. A best explanation approach serves to limit the uncertainty associated with each individual CTD measurement, and to provide a more robust compliance assessment. Together, these lines of

[27] The one-sided confidence bound measures the ability to reliably determine ambient seawater properties within surveys as a whole. They were determined from an analysis of the variability in ambient water-quality data collected during 20 quarterly surveys conducted between 2004 and 2008. Although water-quality observations potentially affected by the presence of wastewater constituents were excluded from the analysis, more than 9,200 remaining observations for each of the six seawater properties accurately quantified the inherent uncertainty in defining the range in natural conditions.

[28] The COP (Appendix I, Page 27, SWRCB 2005) defines a "*significant*" difference as "*a statistically significant difference in the means of two distributions of sampling results at the 95% confidence level.*" Accordingly, COP effluent analyses (Step 9 in Appendix VI, Page 42, Ibid.) are based "*the one-sided, upper 95% confidence bound for the 95th percentile.*"

[29] The 95th-percentile quantified natural variability in seawater properties during the September 2017 survey itself, and was determined from vertical-profiles data unaffected by the discharge.

[30] Thresholds represent limits on wastewater-induced changes to receiving-water properties that significantly exceed natural conditions as specified in the discharge permit and COP. They are determined from the sum of columns to the left and are specific to the September 2017 survey. They do not include the COP allowances specified in the column to the right.

[31] The discharge permit, in accordance with the COP, allows excursions in seawater properties that depart from natural conditions by specified amounts. DO cannot be "*depressed more than 10% from that which occurs naturally,*" and pH cannot be "*changed more than 0.2 units from that which occurs naturally.*" The California Thermal Plan is incorporated into the COP by reference, and restricts temperature increases to less than 2.2ºC.

[32] Permit limits P5 and P6 (Table 6) include specific numerical values promulgated in the RWQCB Basin Plan (1994) in addition to changes relative to natural conditions specified in the COP. The Basin Plan upper-bound pH objective for ocean waters is 8.5, but a more-stringent upper-bound objective of 8.3, which applies to individual beneficial uses, was implemented in the MBCSD discharge permit.

[33] Maximum or minimum value measured during the September 2017 survey, regardless of location within or beyond the ZID

evidence significantly strengthen the conclusion that the discharge fully complied with the permit at the time of the September 2017 survey.

Natural Variability within and beyond the ZID: Although the permit limits only apply to changes in DO, pH, temperature, and transmissivity beyond the ZID, examination of measurements acquired within the ZID frequently provides additional insight into the potential for adverse effects on water quality. However, among all the data collected during the September 2017 survey, salinity was the only seawater property that exhibited a perceptible difference from ambient conditions. Regardless of their association with the plume's effluent salinity signature or their proximity to the diffuser structure, none of the 11,615 temperature, DO, pH, and transmissivity observations exceeded the thresholds of natural variability specified in Table 8. This is apparent from a comparison between the extrema listed in the last data column in Table 8, and the corresponding natural-variability thresholds listed in third data column. For example, ambient seawater temperatures are expected to range as high as 16.58ºC, but the highest measured temperature was 15.82ºC. Similarly, natural excursions in transmissivity are expected to range as low as 64.4%, while the lowest measured transmissivity was 73.2%.

COP Allowances: The COP does not require that wastewater-induced changes remain within the ranges in natural variation listed in the third data column of Table 8, even though these ranges were conservatively used in the data screening process described in previous subsections. Consideration of these COP allowances for receiving-water limits provides an additional safety factor in the compliance evaluation of thermal, DO, and pH excursions.

For pH, the COP and the discharge permit allow changes up to 0.2 pH units from natural conditions, bringing the minimum allowed pH down to 7.7 for the September 2017 survey (fourth data column of Table 8). This limiting value is significantly less than the lowest pH measurement of 7.982 recorded during the September 2017 survey.[34] Similarly, the lowest DO concentration measured during the survey (6.09 mg/L) was well above the lower bound in expected natural variability (4.79 mg/L) and even more so for the less-stringent 10% compliance threshold promulgated by the COP (4.31 mg/L).

Limited Ambient Light Penetration: Although there are no explicit numerical objectives for discharge-related reductions in transmissivity, a numerical limit can be established from the COP requirement that the discharge not result in significant reductions in the transmission of natural light (P4 in Table 6). Because the COP does not specify an allowance beyond natural conditions, the 64.4% threshold on ambient transmissivity variations listed in third data column of Table 8 can be interpreted to constitute a numerical limit.

However, the COP objective for light penetration only applies to a limited subset of the transmissivity measurements. Because little natural light is present beneath the euphotic zone, which extends to twice the Secchi depth, the limit on transmissivity reductions during the September 2017 survey only applies to measurements recorded above 8 m (twice the shallowest Secchi depth listed in Table 4). This immediately eliminates 57% of the transmissivity measurements from further compliance consideration, even though they were included in the screening analysis. Specifically, even if the discharge of wastewater particulates had caused transmissivity measurements collected below the euphotic zone to drop below the numeric compliance threshold, it would not have been of regulatory concern because the penetration of ambient light would not have been affected. This includes measurements collected shortly after discharge near a diffuser port, or those within the naturally turbid BNL above the seafloor, because virtually no natural light was present near the seafloor during the September 2017 survey.

[34] Compliance with COP maximum pH allowance (8.476) is irrelevant because effluent on the day of the survey had a pH of 7.3, which is much lower than the lowest pH measured within the receiving seawater (7.982). Consequently, the presence of effluent constituents could not have induced an increase in pH within receiving waters.

Insignificant Thermal Impact: As with transmissivity, there are no explicit numerical objectives for discharge-related increases in temperature. Nevertheless, a numerical limit can be established for thermal excursions that is based on the requirement that they not adversely affect beneficial uses (P3 in Table 6). Although the COP remains silent regarding allowable temperature changes, it incorporates the California Thermal Plan requirements by reference (COP Introduction §C.3). The Thermal Plan (SWRCB 1972) restricts temperature increases caused by new discharges to coastal water to be less than 2.2°C (4°F). As with DO and pH, a quantitative permit limit on temperature increases can be established by combining the Thermal Plan allowance with the natural variability threshold listed in the third data column of Table 8. Accordingly, increases in temperature caused by the discharge of warm wastewater during the September 2017 survey could be deemed to adversely affect beneficial uses if they exceeded 18.78°C (fourth data column of Table 8). However, none of the 11,615 CTD measurements collected during the survey exceeded 15.82°C (last column in Table 8). As a result, all the measurements remained well within the natural variability thermal threshold (16.58°C), and provided a much larger safety factor for compliance with the numerical limit derived from the Thermal Plan. In reality, temperatures measured within the rising effluent plume were uniformly below that of the surrounding seawater because cooler seawater near the seafloor had been entrained in the plume shortly after discharge. Consequently, any potential thermal impact resulting from the discharge of warm wastewater was almost immediately eliminated upon discharge because the effluent entrained large volumes of much colder seawater near the seafloor.

Directional Offset: Analysis of the directional offset of CTD measurements is useful because wastewater and receiving-seawater properties depart from one another in several predictable ways. Specifically, upon discharge, wastewater is fresher, warmer, more turbid, and less dense than the ambient receiving waters of Estero Bay. As such, the introduction of wastewater constituents will reduce the salinity, density, and transmissivity of the receiving seawater (negative offset), while temperature will be increased (positive offset). Therefore, the reduced temperatures observed in conjunction with the effluent plume during the tow surveys (Figures 9a and 10a) could not have been generated by the presence of warmer wastewater constituents. Instead, they were produced because the plume entrained cooler bottom water shortly after discharge. Similarly, the increased transmissivity observed within the discharge plume during the shallow tow (Figure 10d) could not have been generated by an unacceptably high particulate load within wastewater. In both cases, the directional offsets were opposite of receiving-water impacts expected from the presence of wastewater constituents.

Insignificant Wastewater Particulate Loads: Another independent line of evidence demonstrates that the discharge of wastewater particulates could not have contributed materially to turbidity within the dilute effluent plume, even before completion of the initial mixing process. The effluent suspended-solids concentration measured onshore around the time of the survey was 30 mg/L. After dilution by at least 258 fold, the effluent suspended-solids concentration would have the reduced ambient transmissivity by no more than 0.1%. This small potential decrease in transmissivity is overwhelmed by even the modest 3.5% decrease in ambient transmissivity caused by the natural resuspension of seafloor sediments within the BNL.

Similarly, the MBCSD discharge could not have contributed materially to the observed DO fluctuations. The MBCSD treatment process routinely removes 80% or more of the organic material, as demonstrated by the 39-mg/L BOD measured within the plant's effluent on the day after the survey. That small amount of BOD would have induced a DO depression of no more than 0.022 mg/L after dilution (MRS 2002). In fact, in the absence of a tangible BOD influence, wastewater discharge would actually be expected to increase DO within subsurface receiving waters, rather than decrease it. This is because effluent is oxygenated by recent contact with the atmosphere during the treatment process, whereas receiving waters at depth are typically depleted in DO due to the long absence of atmospheric equilibration within the deep offshore watermass.

Excursions remained within the fixed Basin-Plan Limits: Permit provisions P5 and P6 (Table 6) combine receiving-water objectives from both the COP and the Basin Plan with regard to DO and pH limits. As described previously, the COP requires that DO concentrations outside the ZID not be depressed more than 10% from that which occurs naturally, and restricts pH measurements to those within 0.2 units of that which occurs naturally. In contrast, the Basin-Plan's fixed numerical limits do not provide specific guidance as to how they might change in response to widespread changes in oceanographic conditions unrelated to the discharge. Specifically, the fixed numerical limits restrict DO concentrations outside the ZID to no less than 5 mg/L (P5 in Table 6), and pH levels to the 7.0-to-8.3 range (P6). As such, the fixed Basin-Plan limit on DO is significantly more restrictive than the 4.31 mg/L minimum allowable DO concentration established for the September 2017 survey under COP objectives. Nevertheless, all of the DO measurements complied also with the more conservative Basin-Plan limit on DO reductions. In contrast, the minimum allowable pH (7.0) specified in the Basin Plan was less restrictive than the COP limit (7.7) specified for the September 2017 Survey, so all the pH observations again complied with both regulations.

CONCLUSIONS

The quantitative screening analysis demonstrated that all measurements recorded during the September 2017 survey complied with the receiving-water limitations specified in the NPDES discharge permit. This conclusion was further strengthened by other lines of evidence supporting compliance with the discharge permit. Specifically, although discharge-related changes in seawater properties were observed during the September 2017 survey, the changes were either not of significant magnitude (i.e., they were within the natural range of variability that prevailed at the time of the survey), were measured within the boundary of the ZID where initial mixing is still expected to occur, or were not directly caused by the presence of wastewater constituents within the water column (i.e., were entrainment generated).

Early in the initial mixing process, effluent was being diluted to levels in excess of 248 fold, which is markedly higher than the critical dilution levels predicted by design modeling after completion of the mixing process. Later in the initial mixing process, the plume's depth oscillated vertically about its buoyancy equilibrium level as it was rapidly transported to the south. As these damped buoyancy oscillations dissipated at the completion of the initial dilution process, dilution levels reached 437 fold. All of the measured dilution levels far exceed levels that were predicted by modeling and that were incorporated in the discharge permit as conservative limits on contaminant concentrations within effluent prior to discharge. Lastly, all of the auxiliary observations collected during the September 2017 survey demonstrated that the discharge complied with the narrative receiving-water limits in the discharge permit and the COP. Together; these observations demonstrate that the treatment process, diffuser structure, and the outfall continue to surpass design expectations.

REFERENCES

Davis, R.E., J.E. Dufour, G.J. Parks, and M.R. Perkins. 1982. Two Inexpensive Current-Following Drifters. Scripps Institution of Oceanography, University of California, San Diego, La Jolla, California. SIO Reference No. 82-28. December 1982.

Fischer, H.B., E.J. List, R.C.Y. Koh, J. Imberger, and N.H. Brooks. 1979. Mixing in Inland and Coastal Waters. New York: Academic Press, 482 p.

Kuehl, S.A., C.A. Nittrouer, M.A. Allison, L. Ercilio, C. Faria, D.A. Dukat, J.M. Jaeger, T.D. Pacioni, A.G. Figueiredo, and E.C. Underkoffler 1996. Sediment deposition, accumulation, and seabed dynamics in an energetic fine-grained coastal environment. *Continental Shelf Research*, 16: 787-816.

Marine Research Specialists (MRS). 1998. City of Morro Bay and Cayucos Sanitary District, Offshore Monitoring and Reporting Program, Semiannual Benthic Sampling Report, April 1998 Survey. Prepared for the City of Morro Bay, CA. July 1998.

Marine Research Specialists (MRS). 2002. City of Morro Bay and Cayucos Sanitary District, Supplement to the 2002 Renewal Application For Ocean Discharge Under NPDES Permit No. Prepared for the City of Morro Bay and Cayucos Sanitary District, Morro Bay, CA. July 2002.

Marine Research Specialists (MRS). 2011. City of Morro Bay and Cayucos Sanitary District, Offshore Monitoring and Reporting Program, 2010 Annual Report. Prepared for the City of Morro Bay, California. March 2011.

Marine Research Specialists (MRS). 2012. City of Morro Bay and Cayucos Sanitary District, Offshore Monitoring and Reporting Program, 2011 Annual Report. Prepared for the City of Morro Bay, California. March 2012.

Marine Research Specialists (MRS). 2013. City of Morro Bay and Cayucos Sanitary District, Offshore Monitoring and Reporting Program, 2012 Annual Report. Prepared for the City of Morro Bay, California. March 2013.

Marine Research Specialists (MRS). 2014. City of Morro Bay and Cayucos Sanitary District, Offshore Monitoring and Reporting Program, 2013 Annual Report. Prepared for the City of Morro Bay, California. March 2014.

National Academy of Sciences. 1993. Managing Wastewater in Coastal Urban Areas. National Research Council Committee on Wastewater Management for Coastal Urban Areas, Water Science and Technology Board, Commission on Engineering and Technical Systems. 477 pp.

Regional Water Quality Control Board (RWQCB) - Central Coast Region. 1994. Water Quality Control Plan (Basin Plan) Central Coast Region. Available from the RWQCB at 81 Higuera Street, Suite 200, San Luis Obispo, California. 148p. + Appendices.

Regional Water Quality Control Board (RWQCB) - Central Coast Region and the Environmental Protection Agency (USEPA) – Region IX. 1992a. Waste Discharge Requirements (Order No. 92-67) and Authorization to Discharge under the National Pollutant Discharge Elimination System (Permit No. CA0047881) for City of Morro Bay and Cayucos Sanitary District, San Luis Obispo County.

Regional Water Quality Control Board (RWQCB) - Central Coast Region and the Environmental Protection Agency (USEPA) – Region IX. 1992b. Monitoring and Reporting Program No. 92-67 for City of Morro Bay and Cayucos Sanitary District, San Luis Obispo County (Permit No. CA0047881).

Regional Water Quality Control Board (RWQCB) - Central Coast Region and the Environmental Protection Agency (USEPA) – Region IX. 1998a. Waste Discharge Requirements (Order No. 98-15) and National Pollutant Discharge Elimination System (Permit No. CA0047881) for City of Morro Bay and Cayucos Sanitary District, San Luis Obispo County. 11 December 1998.

Regional Water Quality Control Board (RWQCB) - Central Coast Region and the Environmental Protection Agency (USEPA) – Region IX. 1998b. Monitoring and Reporting Program No. 98-15 for City of Morro Bay and Cayucos Sanitary District, San Luis Obispo County. 11 December 1998.

Regional Water Quality Control Board (RWQCB) - Central Coast Region and the Environmental Protection Agency (EPA) – Region IX. 2009. Waste Discharge Requirements (Order No. R2-2008-0065) and National Pollutant Discharge Elimination System (Permit No. CA0047881) for the Morro Bay and Cayucos Wastewater Treatment Plant Discharges to the Pacific Ocean, Morro Bay, San Luis Obispo County. Effective 1 March 2009.

Sea-Bird Electronics, Inc. (SBE) 1989. Calculation of M and B Coefficients for the Sea-Tech Transmissometer. Application Note No. 7, Revised September 1989.

Sea-Bird Electronics, Inc. (SBE) 1992. SBE 12/22/22/20 Dissolved Oxygen Sensor Calibration and Deployment. Application Note No. 12-1, rev B, Revised April 1992.

Southern California Bight Field Methods Committee (SCBFMC). 2002. Field Operation Manual for Marine Water-Column, Benthic, and Trawl monitoring in Southern California. Technical Report 259. Southern California Coastal Water Research Project. Westminster, CA. March 2002.

State Water Resources Control Board (SWRCB). 1972. Water Quality Control Plan for Control of Temperature in the Coastal and Interstate Waters and Enclosed Bays and Estuaries of California. Revises and supersedes the policy adopted by the State Board on January 7, 1971, and revised October 13, 1971, and June 5, 1972. California Division of Water Quality, Water Quality Planning Unit.

State Water Resources Control Board (SWRCB). 2005. Water Quality Control Plan, Ocean Waters of California, California Ocean Plan. California Environmental Protection Agency. Effective February 14, 2006.

State Water Resources Control Board (SWRCB). 2009. Water Quality Control Plan for Enclosed Bays and Estuaries – Part 1 Sediment Quality. California Environmental Protection Agency. Effective August 22, 2009. sed_qlty_part1.pdf [Accessed 02/26/10].

Suter II, Glenn, W. 2007. Ecological risk assessment, 2nd edition. U. S. Environmental Protection Agency, Cincinnati, Ohio. CRC.

Tetra Tech. 1992. Technical Review City of Morro Bay, CA Section 201(h) Application for Modification of Secondary Treatment Requirements for a Discharge into Marine Waters. Prepared for the U.S. Environmental Protection Agency, Region IX, San Francisco, CA by Tetra Tech, Inc., Lafayette, CA. February 1992.